Published June 18, 2008

ARTICLE

Amino Acid Substitutions in the Pore Helix of GluR6 Control Inhibition by Membrane Fatty Acids

Timothy J. Wilding, Elisabeth Fulling, Yun Zhou, and James E. Huettner

Department of Cell Biology and Physiology, Washington University Medical School, St. Louis, MO 63110

RNA editing at the Q/R site in the GluR5 and GluR6 subunits of neuronal kainate receptors regulates channel inhibition by lipid-derived modulators including the cis-unsaturated fatty acids arachidonic acid and docosahexaenoic acid. Kainate receptor channels in which all of the subunits are in the edited (R) form exhibit strong inhibition by these compounds, whereas wild-type receptors that include a glutamine (Q) at the Q/R site in one or more subunits are resistant to inhibition. In the present study, we have performed an arginine scan of residues in the pore loop of the GluR6(Q) subunit. Amino acids within the range from −19 to +7 of the Q/R site of GluR6(Q) were individually mutated to arginine and the mutant cDNAs were expressed as homomeric channels in HEK 293 cells. All but one of the single arginine substitution mutants yielded functional channels. Only weak inhibition, typical of wild-type GluR6(Q) channels, was observed for substitutions +1 to +6 downstream of the Q/R site. However, arginine substitution at several locations upstream of the Q/R site resulted in homomeric channels exhibiting strong inhibition by fatty acids, which is characteristic of homomeric GluR6(R) channels. Based on homology with the pore loop of potassium channels, locations at which R substitution induces susceptibility to fatty acid inhibition face away from the cytoplasm toward the M1 and M3 helices and surrounding lipids.

INTRODUCTION

Glutamate receptor subunits combine to form tetrameric ion channels in the surface membrane of neurons and several other cell types (Dingledine et al., 1999). Pharmacology of native and recombinant receptors, as well as cDNA sequence analysis, indicates that the 14 homologous ionotropic glutamate receptor subunits contribute to three distinct receptor subfamilies, which are named for the agonists NMDA, α-amino-3-hydroxy-5-methylisoxazole-4-propionic acid (AMPA), and kainate (Dingledine et al., 1999). All of these subunits are thought to share the same transmembrane topology, with the agonist binding site formed by portions of the N-terminal domain and by an extracellular loop between the third and fourth hydrophobic segments, which span the membrane (Wollmuth and Sobolevsky, 2004). For several GluR subunits this agonist binding unit has been crystallized as a soluble fragment (Armstrong et al., 1998; Mayer, 2005). Crystal structure for the transmembrane portion has not yet been reported, but its overall organization is thought to resemble an inverted potassium channel pore (Wo and Oswald, 1995; Wood et al., 1995). In particular, the M2 hydrophobic segment is believed to loop into the membrane from the cytoplasmic side in a manner similar to the extracellular pore loop of bacterial and mammalian K channels (Panchenko et al., 2001; Kuner et al., 2003).

For both AMPA and kainate receptors, previous work (Dingledine et al., 1999) demonstrated that RNA editing at a site within the channel pore controls ion permeation and channel pharmacology. The genes for all AMPA and kainate receptor subunits encode for a glutamine (Q) at this site (Hollmann and Heinemann, 1994); however, mRNAs for AMPA receptor subunit GluR2 and kainate receptor subunits GluR5 and GluR6 can undergo editing at this location to encode for an arginine (R) (Sommer et al., 1991). Channels made up only of unedited subunits exhibit voltage-dependent block by intracellular and extracellular polyamines and are permeable to sodium, potassium, and calcium ions (Dingledine et al., 1999). In contrast, channels that include one or more edited subunits show reduced single channel conductance (Howe 1996; Swanson et al., 1996), reduced permeability to calcium (Köhler et al., 1993; Burnashev et al., 1995, 1996), and weaker block by polyamines (Bowie and Mayer, 1995; Kamboj et al., 1995).

A variety of different ion channels are modulated by direct interactions with cis-unsaturated molecules, including arachidonic acid (AA), docosahexaenoic acid (DHA), and endocannabinoids, which are derived from membrane phospholipids. In some cases, these lipid-derived mediators exert positive modulation, causing potentiation of channel activity (Miller et al., 1992; Fink et al., 1998), whereas other channels are strongly inhibited

Correspondence to James E. Huettner: jhuettner@wustl.edu

The online version of this article contains supplemental material.

Abbreviations used in this paper: AMPA, α-amino-3-hydroxy-5-methylisoxazole-4-propionic acid; AA, arachidonic acid; Con A, concanavalin A; DHA, docosahexaenoic acid; GluR6, glutamate receptor subunit 6; HEK, human embryonic kidney.

The Rockefeller University Press $30.00
J. Gen. Physiol. Cite by DOI:10.1085/jgp.200810009
www.jgp.org/cgi/doi/10.1085/jgp.200810009

Published June 18, 2008

(Poling et al., 1996; Wilding et al., 1998) or exhibit changes in their gating kinetics (Oliver et al., 2004) upon exposure to free AA or DHA. We have previously demonstrated that Q/R site editing controls susceptibility of kainate receptors to inhibition by cis-unsaturated fatty acids (Wilding et al., 2005). In contrast to block by polyamines (Bowie and Mayer, 1995; Kamboj et al., 1995), recombinant kainate receptors only display strong inhibition by fatty acids if all of the subunits are in the edited (R) form; channels that include unedited wild-type subunits resist fatty acid inhibition (Wilding et al., 2005). To explore the basis for kainate receptor inhibition by fatty acids in more detail, we have substituted other amino acids at the Q/R site and generated a series of mutant GluR6(Q) subunits that include an arginine at other locations within the pore loop. Our results show that susceptibility to fatty acid inhibition does not require a positively charged side chain at the Q/R site, or anywhere else within the pore. Instead, our results suggest that vulnerability to fatty acid inhibition depends on the pore loop conformation, which can be modified by specific side chain replacements.

MATERIALS AND METHODS

cDNA Constructs

Wild-type GluR6 cDNA (Egebjerg et al., 1991), provided by S. Heinemann (Salk Institute, La Jolla, CA), was subcloned into pcDNA3 for mammalian expression as previously described (Huettner et al., 1998). Point mutations were made using the QuickChange XL site-directed mutagenesis kit (Stratagene) according to the manufacturer's protocol. Mutation primers were designed to change the coding sequence for single amino acids and simultaneously introduce novel restriction sites, which facilitated identification of mutated subunit cDNAs. Mutations were verified by direct sequencing by the Washington University protein and nucleic acid chemistry laboratory.

Cell Culture and Transfection

Human embryonic kidney (HEK) 293 cells were maintained as previously described (Wilding et al., 1998) in MEM (GIBCO BRL) with 10% FCS (Sigma-Aldrich). Cells were grown to 50–70% confluence in one well of a 12-well plate and transfected using 15 μg of Superfect reagent (QIAGEN) with 1–3 μg of subunit cDNA and 0.5 μg of cDNA for the mouse L3T4 surface antigen to allow for identification of transfected cells. Plasmid DNAs were incubated for 30 min at room temperature with Superfect reagent in 80 μl OptiMEM (GIBCO BRL), and then diluted onto cells growing in 600 μl of MEM plus FCS and 5 mM kynurenic acid. On the next day, cells were incubated for ~10 min with 1 mg ml^{-1} protease XXIII (Sigma-Aldrich), and then dissociated and replated at lower density on 35-mm culture dishes that had been coated with a thin layer of nitrocellulose to promote cell attachment. Physiological recordings were made 24–48 h after replating. Cells were incubated for 30 min with phycoerythrin-conjugated monoclonal anti-L3T4 (BD Biosciences). Isolated cells that were labeled with the anti-L3T4 antibody were targeted for recording.

Electrophysiology

Cultured cells were perfused at 1 ml min^{-1} with Tyrode's solution (in mM): 150 NaCl, 4 KCl, 2 $MgCl_2$, 2 $CaCl_2$, 10 glucose, 10 HEPES, pH adjusted to 7.4 with NaOH. Whole-cell electrodes filled with internal solution containing (in mM) 140 Cs glucuronate, 10 EGTA, 5 CsCl, 5 $MgCl_2$, 5 ATP, 1 GTP, and 10 HEPES, pH adjusted to 7.4 with CsOH. For most experiments, electrodes had an open tip resistance of 1–5 MOhm. Currents were recorded with an Axopatch 200A amplifier, filtered at 1–2 kHz (-3dB, 4 pole Bessel), and digitized at 5–10 kHz. For many experiments cells were preincubated with 2 μM concanavalin A to increase steady-state agonist responses (Huettner, 1990). Agonist solutions were delivered as previously described (Wilding et al., 1998) from an eight-barreled local perfusion pipette. For rapid solution exchange, the drug reservoirs were maintained under static air pressure (~10 p.s.i.) and flow was controlled by computer-gated electronic valves. Despite recognized limitations on the speed of solution exchange in the whole cell mode (tau ~5-15 ms), whole-cell recordings were used to analyze desensitization because of the small maximal current amplitude observed for a number of the mutant subunits.

Fatty acids stock solutions (50 mM) were prepared in DMSO and stored at −80°C in aliquots under argon gas; fresh dilutions were prepared each day for recording. The effect of DHA was quantified as the ratio of agonist-evoked current immediately after 2–3 min treatment with 15–50 μM fatty acid in external solution to the control current immediately before DHA exposure. Currents inhibited by DHA recovered to the control amplitude after a 3–5-min wash with external solution containing 0.1% BSA (Wilding et al., 1998, 2005). Rectification index was calculated as the ratio of agonist-gated slope conductance at +40 and −80 mV. To compare the relative permeability of wild-type and mutant channels to chloride ions (Burnashev et al., 1996) we determined the shift in reversal potential for agonist-gated current in a low chloride external solution (160 mM Na-glucuronate, 10 mM HEPES, 2 $CaCl_2$, pH to 7.4 with NaOH) as compared with our normal extracellular solution for drug delivery (160 NaCl, 10 HEPES, 2 $CaCl_2$, pH to 7.4 with NaOH).

Fluctuations in agonist-gated currents were evaluated as previously described (Huettner, 1990) for data recorded during bath applications of 10 μM kainate. Steady-state current variance was calculated over 1-s time intervals after first subtracting a straight line to correct for steady amplitude changes. Plots of variance (σ^2) versus mean current (I) were fit with the equation $\sigma^2 = i * I - I^2/N$ (Sigworth, 1980; Traynelis and Jaramillo, 1998) by adjusting the parameters i and N, which are the estimated unitary current amplitude (i) and the estimated number of channels (N), respectively. Open probability (P_o) was estimated as the ratio $P_o = I_{max}/(i * N)$, where I_{max} is the maximal mean whole-cell current (Sigworth, 1980).

Single Channel Recording and Analysis

Pipettes used for single channel recordings were coated with sylgard and fire polished to an open tip resistance of 5–10 MOhm. Outside-out patches pulled from transfected HEK cells were superfused with external solution (160 NaCl, 10 HEPES, 2 $CaCl_2$, pH to 7.4 with NaOH) containing either 0.1% BSA (control) or 30 μM kainate or 30 μM kainate plus 15 μM DHA. For most patches it was possible to cycle through these three solutions repeatedly, demonstrating that the currents evoked by kainate were reproducible and that the effect of DHA, if any, was consistent and reversible. Patches that exhibited unitary currents when equilibrated in control solution were discarded. Single channel currents were recorded with an Axopatch 200A amplifier in the patch (integrating) mode, filtered at 1–2 kHz (−3dB, 4 pole Bessel) and digitized at 10–20 kHz. Patch recordings were analyzed with P-clamp (Axon instruments) to obtain distributions of unitary current amplitudes and open and shut durations. Sojourns with duration >200 μs were accepted as transitions between open and shut levels and dwell times were corrected by post-hoc interpolation.

Published June 18, 2008

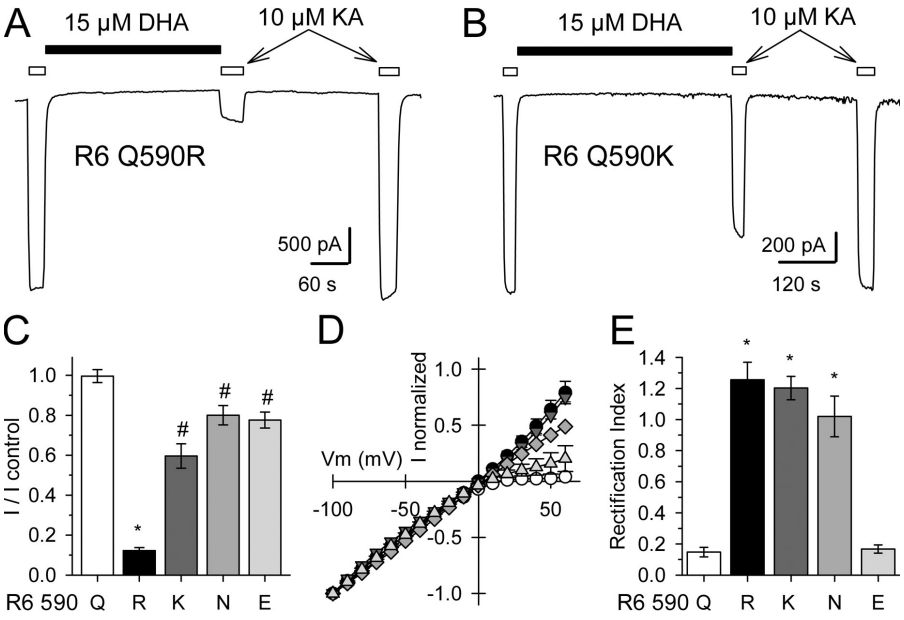

Figure 1. Intermediate inhibition of homomeric channels substituted at the Q/R site. (A) Whole-cell current evoked by 10 μM kainate (open bars) before and after exposure to 15 μM DHA (closed bar) in a Con A–treated HEK293 cell transfected with GluR6 Q590R cDNA. (B) Current evoked by kainate in a Con A–treated cell that was transfected with cDNA encoding GluR6 Q590K before and after exposure to DHA. (C) Current evoked by 10 μM kainate immediately after exposure to 15 μM DHA plotted as a fraction of control current before DHA. #, inhibition of GluR6 Q590K ($n = 6$ cells), Q590N ($n = 7$) and Q590E ($n = 10$) was significantly different from 590Q ($n = 32$) and 590R ($n = 26$). (D) Currents evoked by 10 μM kainate as a function of holding potential for homomeric GluR6 Q590 (open circles); Q590R (filled circles); Q590K (inverted triangles); Q590N (diamonds); Q590E (upright triangles). (E) Rectification index (slope conductance ratio at +40 and −80 mV) for the five Q/R site variants ($n = 14$ Q; 19 R; 15 K; 10 N; 10 E cells). *, significantly different from Q590.

Amplitude histograms were fitted with Gaussians and the unitary current amplitude calculated from the difference between peaks. Histograms of the logarithm of open and shut durations were plotted using a square root transformation and normalization to the total event count. Distributions were fitted with a combination of exponential probability density functions. The minimal number of exponential components required for an adequate fit was determined by an F-test on residuals.

Consistent with previous work on GluR6(Q) channels (Swanson et al., 1996) and native kainate receptors (Smith and Howe, 2000; Gebhardt and Cull-Candy, 2006) agonist applications evoked channel openings to multiple subconductance levels for all of the mutant subunits tested. The T576R substitution was selected for detailed analysis because the majority of openings were to one main conductance level. Patches used for analysis displayed no more than two or three channels open simultaneously at any point during the recording. Open and shut periods were evaluated over 5–10-s recording segments when it appeared that only one channel was active. Open periods included dwell time at any subconductance level, except the closed level.

Molecular Modeling

Sequence alignments and homology modeling were performed using the Modeller program (Sali and Blundell, 1993) available at http://salilab.org/modeller/modeller.html. Preliminary analysis indicated that use of multiple templates yielded predictions with lower overall energy. The homology modeling was restricted to monomeric templates and ignored possible constraints imposed by the tetrameric organization of subunits within pore-loop channels.

Homology model figures were prepared with Swiss Pdb Viewer and POV-Ray.

Online Supplemental Material

The online supplemental material contains six figures (available at http://www.jgp.org/cgi/content/full/jgp.200710009/DC1). Fig. S1 A illustrates the region of GluR6 that was modeled and the alignment to segments of four different potassium channel subunits: KcsA, PDB entry: 1R3J (Zhou and MacKinnon, 2003); KirBac1.1, PDB: 1P7B (Kuo et al., 2003); KvAP, PDB: 2A0L (Lee et al., 2005); Kv1.2, PDB: 2A79 (Long et al., 2005) that were used as simultaneous templates. Fig. S2 presents views of the modeled GluR6 subunit segment as a homotetramer, together with lipids from the crystal structure of Long et al. (2007). Fig. S3 shows that edited residues in TM1 do not affect DHA inhibition. Fig. S4 shows that DHA inhibition correlates with mean control current amplitude. Fig. S5 presents statistical analysis of control current amplitude for each mutation in Fig. S4. Fig. S6 shows that DHA inhibition does not correlate with the extent or time course of whole-cell current desensitization.

RESULTS

Amino Acid Substitutions at the Q/R Site

Our previous work showed that homomeric recombinant kainate receptors formed by the edited GluR6(R) subunit exhibit potent noncompetitive inhibition by cis-unsaturated fatty acids, whereas homomeric or heteromeric channels that included unedited GluR6(Q) subunits are resistant to fatty acid inhibition (Wilding et al., 1998, 2005). We first analyzed the specificity of the Q/R site to this effect by substituting glutamine (Q590) with the positively charged lysine (K), as in arginine (R), and with the negatively charged but similarly sized glutamate (E). We also tested an asparagine (N) substitution because an N resides at the homologous position of all NMDA receptor NR1 and NR2 subunits (Moriyoshi et al., 1991, Monyer et al., 1992), and NMDA

Published June 18, 2008

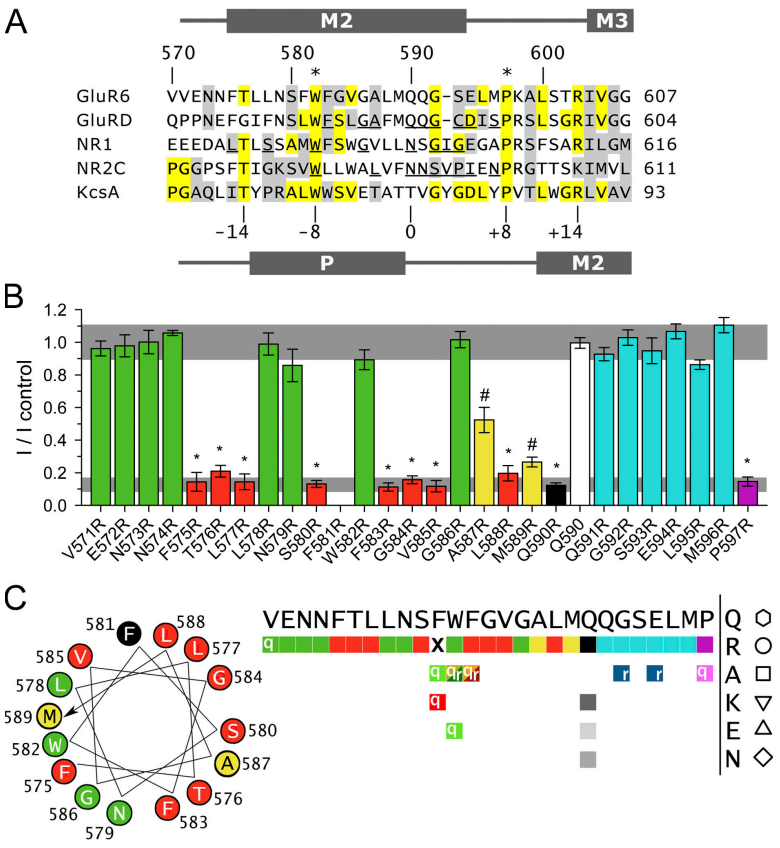

Figure 2. Arginine scan of the GluR6 pore loop. (A) Pore loop sequence alignment for kainate receptor subunit GluR6 (Egebjerg et al., 1991) with AMPA (GluRD; Keinänen et al., 1990) and NMDA receptor (NR1, Moriyoshi et al., 1991; and NR2C, Kutsuwada et al., 1992; Monyer et al., 1992) subunits and with the bacterial potassium channel KcsA (Schrempf et al., 1995). Residue numbering for the GluR6 mature protein is shown above the alignment. The Q/R editing site is located at position 590. Numbers to the right of the alignment denote the sequence position of the final illustrated residue. Yellow shading highlights residues identical to KcsA; gray shading indicates conservative substitutions relative to KcsA. Asterisks label W (−8) and P (+8) residues common to all rat ionotropic glutamate receptor subunits. Underlined residues of GluRD (Kuner et al., 2001), NR1, and NR2C (Kuner et al., 1996), when substituted with cysteine, are accessible to modification by methanethiosulfonate reagents applied from the cytoplasmic side of the membrane. Shaded boxes above the alignment indicate residues contributing to putative M2 and M3 membrane-associated segments based on glutamate receptor subunit hydropathy analysis (Dingledine et al., 1999). Below the alignment is a diagram illustrating residues that contribute to the P and M2 α helical domains of the KcsA crystal structure (Doyle et al., 1998). (B) Current evoked by 10 μM kainate immediately after exposure to 15 μM DHA plotted as a fraction of control current before DHA. All recordings from HEK293 cells expressing homomeric wild-type unedited GluR6(Q) (open bar, n = 32 cells), wild-type edited GluR6(R) (black bar, n = 26), or mutant GluR6(Q) subunits bearing the indicated arginine substitutions (n = 7–19 cells per construct). *, significantly different from Q590, one-way ANOVA on ranks, $P < 0.05$ by Dunn's method of post-hoc comparison to control (red bars in the pore loop helix; violet bar in the M2-M3 loop). #, significantly different from both 590Q and Q590R, rank sum test, $P < 0.0001$ (yellow bars). Horizontal shaded gray bars indicate the 99% confidence intervals for GluR6(Q) and GluR6(R). (C, left) Helical wheel representation of residues F575 through M589 viewed from the carboxy-terminal end of the helix. Locations where R substitution to GluR6(Q) did (red) or did not (green) allow for strong DHA inhibition lie along opposite faces of the helix. (C, right) Color code and symbol code for residue substitutions throughout the paper. Substitutions upstream of the Q/R site are colored shades of red or yellow for strong or intermediate DHA inhibition, respectively, or colored green for lack of inhibition. R and A substitutions at P597 that enhance DHA inhibition of GluR6Q are colored violet. Other downstream locations that do not enhance DHA inhibition are blue. Lowercase q and r in white text indicate the editing status at the Q/R site for each construct.

receptor-mediated currents are potentiated by AA (Miller et al., 1992) and DHA (Nishikawa et al., 1994).

As illustrated in Fig. 1, homomeric GluR6 Q590K channels resisted strong inhibition by DHA typical of GluR6(R), and instead displayed an intermediate level of inhibition, which was greater than observed for GluR6(Q) ($P < 0.001$) yet less than GluR6(R) ($P < 0.0001$) (Fig. 1, A–C). The GluR6 Q590N and Q590E substitutions also resulted in intermediate levels of inhibition between GluR6(Q) and GluR6(R), albeit weaker than for GluR6 Q590K ($P < 0.02$). Thus, an R side chain at the Q/R site yields stronger inhibition than other positive (K) or negative (E) substitutions. In addition, exposure of GluR6 Q590N channels to DHA did not cause potentiation of current as occurs for NMDA receptor channels (Miller et al., 1992; Nishikawa et al., 1994), demonstrating that homomeric expression of N at the Q/R site is not sufficient to account for NMDA receptor potentiation by DHA.

Arginine Substitutions in the Pore Loop of GluR6(Q)

To test whether arginine substitution at other locations in the pore loop could support potent inhibition of GluR6(Q), we generated a series of single point mutations that scanned residues from V571 through P597 (Fig. 2 A). All of these mutant subunits yielded functional channels though currents for the F581R substitution were too small for detailed analysis (−41 ± 9.3 pA peak current evoked by 10 μM kainate, n = 24 cells). Importantly, several of the mutant channels displayed strong inhibition by DHA (Fig. 2 B), which demonstrates that positive charge at residue 590 is not absolutely required for fatty acid inhibition. Residue substitutions that conferred susceptibility to DHA were predominantly located upstream of the Q/R site, whereas subunits with arginine substitutions at the six consecutive positions downstream of the Q/R site were not inhibited by DHA.

Published June 18, 2008

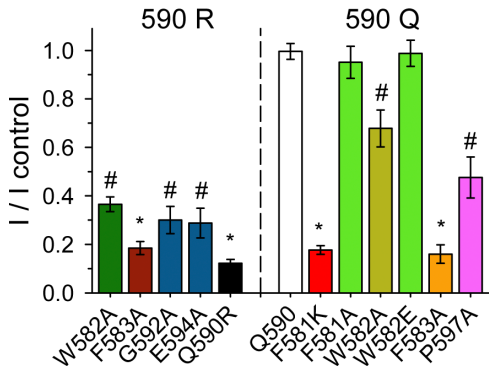

Figure 3. Positive charge is not required for strong DHA inhibition. Whole-cell current evoked by 10 μM kainate immediately after exposure to 15 μM DHA plotted as a fraction of control current before DHA. All recordings from HEK293 cells expressing homomeric wild-type unedited GluR6(Q) (open bar), wild-type edited GluR6(R) (black bar), or mutant GluR6(Q) or (R) subunits bearing the indicated substitutions (n = 5–27 cells per construct). The alanine substitutions caused minimal reduction in DHA inhibition of GluR6(R), but F583A dramatically increased DHA inhibition of GluR6(Q).

Based on studies of accessibility to cysteine-modifying reagents (Kuner et al., 1996, 2001), and on analogy with the pore loop crystal structure of homologous potassium channels (Panchenko et al., 2001; Kuner et al., 2003), the Q/R site is believed to reside at the apex of the AMPA and kainate receptor subunit pore loops. Residues downstream of the Q/R site are thought to constitute the narrow selectivity filter, which is followed by a short cytoplasmic loop leading into the M3 transmembrane helix (Fig. S1 B, available at http://www.jgp.org/cgi/content/full/jgp.200810009/DC1). Among the downstream mutants tested, only the GluR6(Q) P597R mutant was inhibited by DHA. Sequence alignment indicates that a proline residue is highly conserved at this location among pore loop–containing channels (Fig. 2 A), including all ionotropic glutamate receptor subunits and the majority of potassium-selective channels (Kuner et al., 2003). Because structural constraints on proline bond angles might help to stabilize the pore loop configuration, we tested whether substitution of GluR6(Q) with an uncharged alanine residue at location 597 might also confer sensitivity to DHA. As described below (Fig. 3), we observed that homomeric GluR6(Q) P597A channels displayed intermediate inhibition by DHA, weaker than observed for GluR6(Q) P597R but significantly stronger than for wild-type GluR6(Q). Thus, positive charge at location 597 is not required to allow for DHA inhibition.

In contrast to the observation that most downstream arginine substitutions were not permissive for DHA inhibition of GluR6(Q), mutations upstream of the Q/R site displayed a periodic change in sensitivity to DHA. Arginine substitutions at positions 4, 8, 11, 12, and 16–19 residues upstream of the Q/R site showed no increased inhibition by DHA as compared with wild-type GluR6(Q), whereas replacing almost any of the other upstream amino acids (−1 to −15) with R resulted in inhibition that was essentially equivalent to wild-type GluR6(R) channels. Substitution of A587 or M589 (positions −3 and −1 relative to the Q/R site, respectively) yielded channels with an intermediate level of DHA inhibition. The upstream amino acids are believed to form a helix that begins ∼15 residues before the Q/R site, and which is preceded by a cytoplasmic loop arising from the end of TM1 (Panchenko et al., 2001; Kuner et al., 2003). Interestingly, all of the locations at which R substitution failed to increase sensitivity to DHA are predicted to lie along one face of the pore loop helix (Fig. 2 C). Studies of accessibility to cysteine-modifying methanethiosulfonate (MTS) reagents (Kuner et al., 1996, 2001) indicate that this face of the helix is oriented such that these residues are accessible to modification and therefore likely to be exposed to the cytoplasm. Thus, R substitution enhances DHA inhibition at residues that point away from the cytoplasm, toward the transmembrane helices or surrounding lipids (Fig. S2), where they may alter the pore loop conformation in such a way as to render channels susceptible to modulation. Importantly, substitutions that allow for strong inhibition of GluR6(Q) are spread along the entire length of the predicted pore loop helix but do not extend far into the presumed cytoplasmic loop that precedes M2. These results raise the interesting possibility that the difference in DHA susceptibility between wild-type edited (R) and unedited (Q) channels may primarily reflect alterations in the overall conformation of the pore loop helices within the channel tetramer, rather than a specific interaction involving the side chain of the Q/R site.

Other Substitutions in the Pore Loop of GluR6(R) and GluR6(Q)

In a study of polyamine block of homomeric GluR6(Q) channels, Panchenko et al. (2001) observed a substantial reduction in blocker affinity when alanine (A) was substituted for residues at several locations within the pore loop including F583, G592, and E594. Similarly, Williams and colleagues (Williams et al., 1998; Kashiwagi et al., 2002) observed changes in permeation and a reduction in Mg and organic ion block of NMDA receptors for substitutions at residues homologous to W582 and Q591. To begin testing whether these residues are important for fatty acid inhibition we prepared four mutant versions of the GluR6(R) subunit with single alanine substitutions at the following locations: W582A, F583A, G592A, and E594A (Fig. 3). In contrast to polyamine block of GluR6(Q), which is dramatically reduced by all four of these substitutions (Panchenko et al., 2001), we observed only modest reduction in DHA inhibition of GluR6(R). Thus, substitutions that limit channel pore block by polyamines (Panchenko et al., 2001) in GluR6(Q), or by Mg (Williams et al., 1998) and

Published June 18, 2008

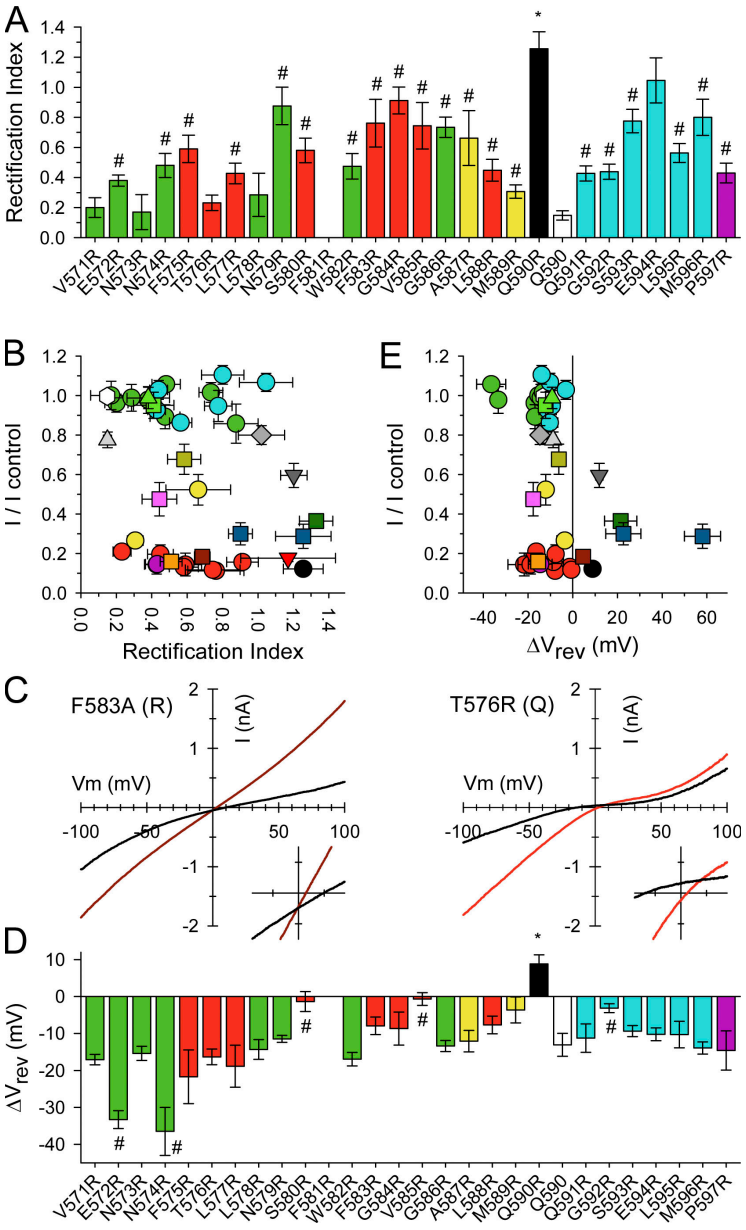

Figure 4. Permeation properties do not correlate with DHA inhibition. (A) Rectification index (slope conductance ratio at +40 and −80 mV) for currents recorded in HEK cells expressing homomeric wild-type GluR6(Q) (open bar), GluR6(R) (black bar), or the indicated R substitution mutants of GluR6(Q). (B) Plots of fractional inhibition by DHA (I/I control) versus rectification index for all of the pore loop mutations (n = 4–24 cells per construct; see color and symbol codes in Fig. 2 C). (C) Current–voltage relations for kainate-evoked current recorded for GluR6(R) F583A (left) and GluR6(Q) T576R (right) as the holding potential was ramped from −100 to +100 mV in control (NaCl, red curves) and low chloride (Na-glucuronate, black curves) external solutions (see Materials and methods). Inserts expand both axes to display the positive and negative shifts in reversal potential for F583A and T576R substitutions, respectively. (D) The change in reversal potential (ΔVrev) of kainate-evoked current upon substitution of Na-glucuronate for extracellular NaCl is plotted for the indicated pore loop substitution mutants. (E) Fractional inhibition by DHA (I/I control) plotted versus ΔVrev in kainate-evoked current with glucuronate substitution (n = 3–17 cells per construct).

MK-801 (Kashiwagi et al., 2002) in NMDA receptors, do not prevent inhibition of GluR6(R) by DHA.

Although W582A and F583A did not act as loss of function mutations for DHA inhibition of GluR6(R), we tested whether these same substitutions might induce gain of function for DHA inhibition of GluR6(Q). Importantly, alanine substitution for F583 resulted in strong inhibition of GluR6(Q) to a level comparable to GluR6(R) (Fig. 3), whereas W582A exhibited an intermediate level of inhibition and W582E, as for GluR6(Q) W582R (Fig. 2), showed no increase in DHA inhibition. As noted above, alanine substitution at position P597 of GluR(Q) also yielded channels with intermediate inhibition (Fig. 3). Collectively, these results show that insertion of positive charge within the pore loop helix is not required for strong inhibition by DHA. Because homomeric GluR6(Q) F581R yielded currents that were too small to test for DHA inhibition (see above), we also evaluated F581K and F581A. As shown in Fig. 3, DHA did not affect currents mediated by GluR6(Q) F581A but inhibited F581K to the same extent as GluR6(R). Thus, replacing hydrophobic F581 with a positively charged lysine supports DHA inhibition similar to adjacent S580R and nearby F583R, whereas the smaller uncharged side chain of alanine is particularly conducive to DHA inhibition at location F583, with little or no effect when substituted at positions W582 or F581, respectively.

Editing Sites in M1

In addition to the Q/R site, GluR6 can be edited at two locations in the first transmembrane domain (Köhler et al., 1993). Genomic DNA encodes for valine (V) at

Published June 18, 2008

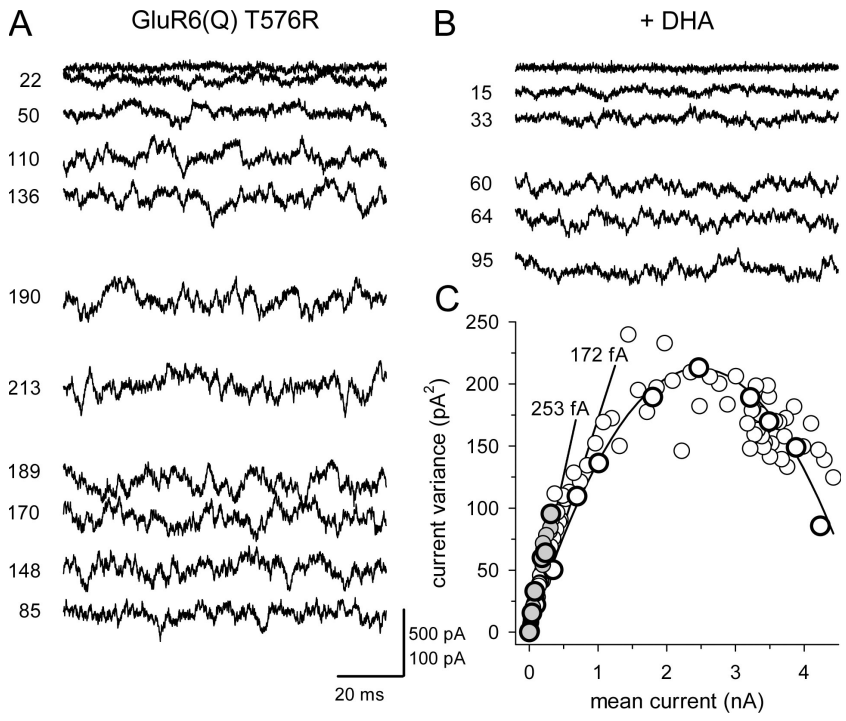

Figure 5. Inhibition by DHA is not restricted to channels with low unitary conductance. Whole-cell currents evoked during bath application of 10 μM kainate before (A) or after (B) application of 15 μM DHA. Numbers to the left of each trace report the variance (σ^2) relative to control external solution before the onset of kainate (top trace in each column). Bar, 100 pA for current traces in A and B; 500 and 100 pA for mean current offsets in A and B, respectively. (C) Plot of current variance versus mean current for the cell illustrated in A and B. Open circles recorded before and filled circles after exposure to DHA. Symbols with thickened borders correspond to the traces illustrated in A and B. The parabolic smooth curve is the best fit of $\sigma^2 = i * I - I^2/N$, where i is the estimated unitary current amplitude and N is the estimated number of channels. The straight line with slope of 172 fA is tangent to the parabolic smooth curve and corresponds to the estimated i from the parabolic fit. The straight line with slope of 253 fA is the best linear fit of the points recorded after exposure to DHA.

position 536 and cysteine (C) at position 540, but GluR6 mRNA can be edited to substitute isoleucine (I) at location 536 and tyrosine (Y) at 540, respectively (Köhler et al., 1993). Our previous studies (Wilding et al., 1998 & 2005) and the experiments in Fig. 1–3 used channels homomeric for V536 and C540. To test whether the naturally occurring V536I or C540Y substitutions could affect susceptibility to fatty acid inhibition, we prepared single point mutations of GluR6(R) and GluR6(Q). As shown in Fig. S3, neither of the substitutions reduced DHA inhibition of GluR6(R) or increased inhibition of GluR6(Q), suggesting that in vivo editing at these locations will have little effect on channel modulation.

Lack of Correlation between Permeation Properties and DHA Inhibition

As shown in Fig. 1 (C and E), differences in rectification induced by amino acid substitutions at the Q/R site (Panchenko et al., 1999) did not correlate with susceptibility to DHA. To test whether there was any consistent relationship between channel permeation properties and DHA inhibition, we calculated rectification indices from current–voltage relations for all of the M2 pore loop mutations (Fig. 4, A and B). For these experiments, voltage was ramped between −100 to +100 mV at 1 mV/ms in a sawtooth pattern. Although several of the R substitution mutants of GluR6(Q) displayed reduced rectification relative to wild-type GluR6(Q), there was no significant correlation between rectification and relative inhibition by DHA. These results indicate that sensitivity to DHA is totally unrelated to configurations of the channel that allow for pore occupancy by polyamines, which is the mechanism of inward rectification (Bowie and Mayer, 1995; Kamboj et al., 1995).

In addition to rectification, we also tested for chloride permeation (Burnashev et al., 1996) through wild-type and mutant channels by substituting sodium glucuronate for extracellular NaCl (Fig. 4, C–E). Wild-type GluR6(R), which is permeable to Cl^- (Burnashev et al., 1996), and five additional mutants (GluR6 Q590K and the W582A, F583A, G592A, and E594A substitutions of GluR6(R)) displayed a +5 to +58-mV shift in reversal potential when glucuronate was substituted for external chloride. This change is consistent with reduction in net outward current by elimination of inward flux of negatively charged chloride ions. Importantly, every channel with positively charged side chains at the Q/R site, and only these channels, exhibited a positive shift in reversal potential upon glucuronate substitution. In contrast, glucuronate substitution shifted the reversal potential for GluR6(Q) and all of the other mutants by −1 to −36 mV relative to extracellular NaCl, possibly owing to reduced Na^+ activity in equimolar glucuronate relative to Cl. Taken together, these results demonstrate that susceptibility to DHA inhibition does not depend on the ability of the channel to conduct chloride ions. In addition, our results suggest that a positively charged side chain at the Q/R site is particularly effective in supporting chloride permeation relative to any other location within the pore loop.

DHA Inhibition Correlates with the Mean Amplitude of Whole-Cell Current

In contrast to the lack of correlation between DHA inhibition and channel rectification or chloride permeation,

Published June 18, 2008

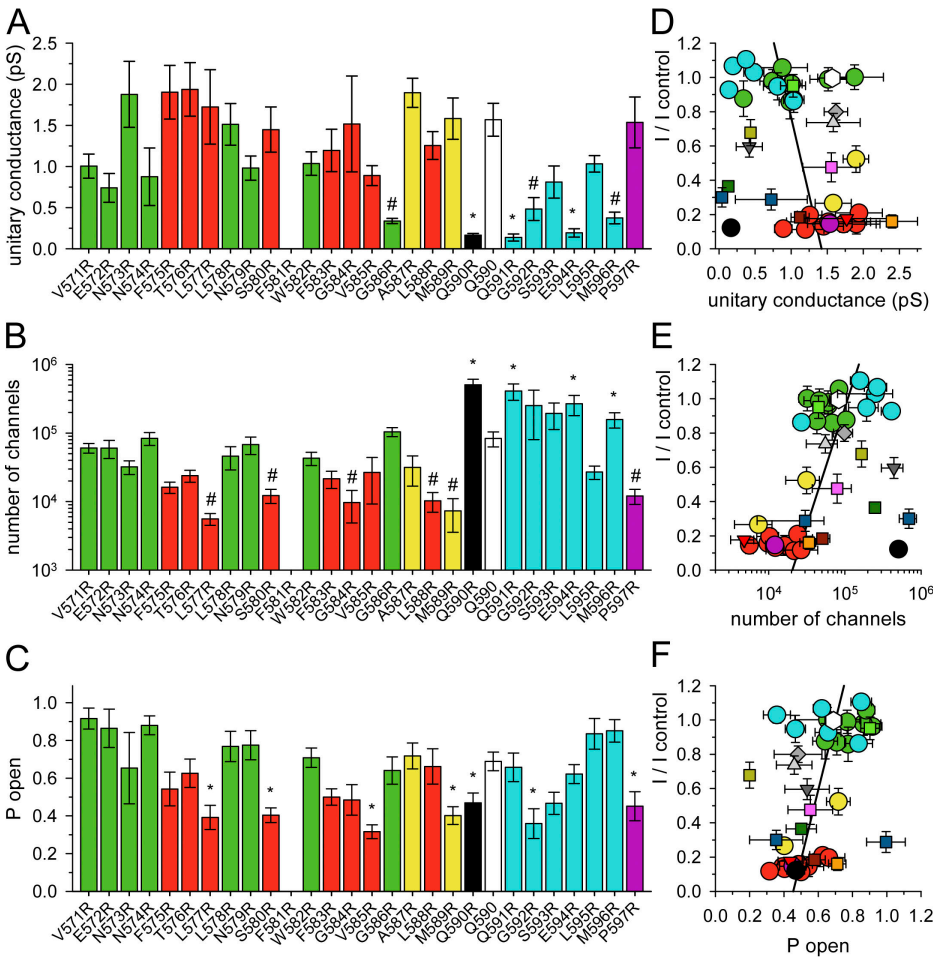

Figure 6. Whole-cell fluctuation analysis highlights the similarity of GluR6(R) with substitution mutants in the downstream selectivity filter. (A and B) Unitary current and number of channels were estimated from the best fits of $\sigma^2 = i * I - I^2/N$ (where i is the estimated unitary current amplitude and N is the estimated number of channels) to plots of variance (σ^2) versus mean current (I) as in Fig. 5 (n = 3–21 cells per construct). Unitary conductance was calculated as unitary current/holding potential. (C) Popen was estimated from the maximal whole-cell current divided by the product ($i \times N$). *, significantly different from GluR6(Q); #, significantly different from both GluR6(Q) and GluR6(R). (D–F) Plots of fractional inhibition by DHA (I/I control) versus estimated unitary conductance (D), log estimated number of channels (E), and estimated open probability (F). For all three parameters the Pearson product moment correlation coefficient was significant: g, −0.343, P = 0.03; log N, 0.490, P < 0.002; Popen, 0.481, P < 0.002. Best fit straight lines through all the data points are drawn in each plot. In D and E, note that substitutions with R at the Q/R site exhibit lower unitary conductance and higher estimated number of channels than GluR6(Q) substitution mutants with comparable levels of DHA inhibition.

we observed a significant negative correlation between inhibition by DHA and the mean amplitude of control whole-cell current, recorded before DHA was applied. As mean control current increased, relative inhibition by DHA decreased (Fig. S4 B). One possible way to explain this relation would be if inhibition was reduced in cells with very large currents because the number of channels exceeded the effective local concentration of DHA within the membrane. To test this possibility, we asked whether inhibition by DHA was correlated with control current amplitude on a cell-by-cell basis for each mutation. As illustrated in Fig. S4 C, there was no consistent relationship between the amplitude of control current and the extent of DHA inhibition among all of the cells expressing a specific cDNA construct. For the 41 genotypes tested, one mutation displayed significant negative correlation (GluR6(Q) M596R) whereas three were positively correlated (GluR6(R) W582A, GluR6(Q) V571R, and L577R); correlation in the remaining 37 genotypes was not significant (P > 0.05) (Fig. S5). These results suggest that inhibition by DHA does not depend on the absolute number of channels in the membrane, which most likely underlies the range of current amplitudes for any given subunit genotype; but, they leave open the possibility that subunits that are susceptible to DHA may, on average, be expressed at lower density. Because whole-cell current amplitude (I) is the product of channel number (N), unitary current (i), and open probability (p_o): $I = i \times N \times p_o$, differences in mean current amplitude from one substitution mutant to the next could reflect differences in i, p_o, N, or some combination of these parameters.

Fluctuation Analysis

Homomeric GluR6(R) receptors have a very low estimated unitary conductance (~225–260 fS; Howe, 1996; Swanson et al., 1996), which precludes a detailed single channel analysis of DHA inhibition at wild-type receptors. To gain insight into the underlying differences between channels that were susceptible versus resistant to inhibition by DHA, we used analysis of whole-cell current fluctuations evoked by a saturating concentration of kainate to estimate the unitary current amplitude, open probability, and N (Huettner, 1990). For several of the substitution mutants, we evaluated kainate-evoked

Published June 18, 2008

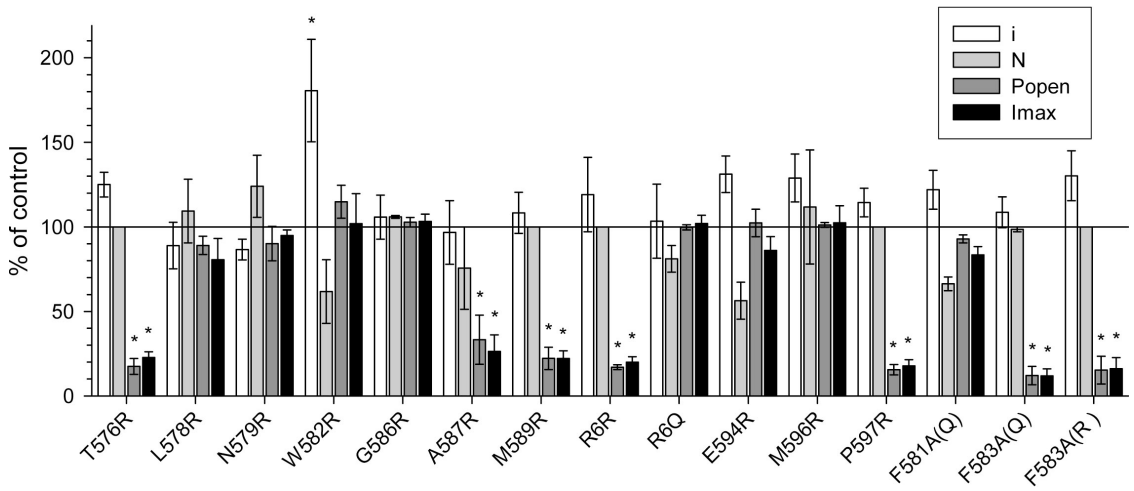

Figure 7. DHA reduces estimated Popen. Whole-cell current fluctuations were analyzed in the absence and presence of DHA as illustrated in Fig. 8. Estimated values for i, N, and Popen and measured values for maximal current in the presence of DHA are plotted as a percent of the values in control ($n = 4$–9 cells per construct). For substitutions that dramatically reduced Popen the unitary current was estimated from a linear fit to the variance versus mean data and N was assumed to be unchanged by DHA application. *, significantly different from control.

current fluctuations both in control external solution and after equilibration with DHA. Fig. 5 presents a representative example from the GluR6(Q) T576R substitution mutant of currents recorded before (Fig. 5 A) and after (Fig. 5 B) exposure to DHA. The plot of variance versus mean current (Fig. 5 C), and the summary plots for the other constructs tested (Fig. 6 and 7), provides evidence for several important conclusions. First, exposure to DHA does not reduce the estimated unitary conductance but does significantly lower the estimated open probability to an extent sufficient to account for the reduction in whole-cell current amplitude by DHA (Fig. 7). This result supports the idea that DHA primarily affects channel gating, not the flux of ions through channels that are open. Second, the majority of GluR6(Q) substitution mutants, including many that are strongly inhibited by DHA, exhibit estimated unitary conductance levels that are significantly larger than wild-type GluR6(R) channels. This result indicates that susceptibility to DHA inhibition is not restricted to channels with small unitary conductance typical of wild-type GluR6(R). Third, comparison of the estimated i and N values for GluR6(R) to the R substitution mutants of GluR6(Q) (Fig. 6, A–C) suggests that for these two parameters GluR6(R) more closely resembles the mutants with substitutions downstream in the loop that forms the selectivity filter than mutants with substitutions in the upstream helix. Thus, GluR6(R) and GluR6(Q) Q591R and E594R display the lowest estimated unitary conductance and the highest estimated number of channels. In contrast, upstream R substitutions in the pore helix that confer susceptibility to DHA inhibition are predominantly associated with lower estimated channel numbers and higher estimated unitary conductance values than adjacent substitutions that resist inhibition by DHA.

Estimated p_o values spanned a narrower range (0.21–0.98) than for i and N (minimum to maximum differences of ~5, ~57, and ~145-fold for p_o, i, and N, respectively), but in this case the majority of subunits inhibited by DHA, including GluR6(R), exhibited relatively lower estimated p_o, whereas most of the subunits that were resistant to DHA, including GluR6(Q), exhibited higher p_o values. Thus, substitutions with lower open state equilibrium stability (lower p_o) are more likely to be susceptible to DHA, which causes inhibition by further reducing p_o. Collectively, the summary plots in Fig. 6 (D–F) suggest that the correlation we observed between control current amplitude and resistance to DHA (Fig. S4 B) can arise in two different ways. Subunits with an R at the Q/R site exhibit a relatively high estimated number of channels with very low unitary conductance and a relatively low p_o, whereas subunits with a Q at the Q/R site that are inhibited by DHA exhibit a relatively large unitary conductance but a low estimated number of channels and relatively low p_o.

Single Channel Recordings

The results in Fig. 6 A suggested that it might be possible to analyze DHA inhibition of unitary currents through GluR6(Q) channels with R substitutions in the upstream pore helix. After preliminary recordings from several different mutants (see Materials and methods) we focused on GluR6(Q) T576R because this substitution yielded well-resolved channels and the majority of openings were to one main conductance level (Fig. 8 B). Consistent with our analysis of whole-cell current fluctuations (Figs. 5–7), exposure to DHA did not alter the amplitude

Published June 18, 2008

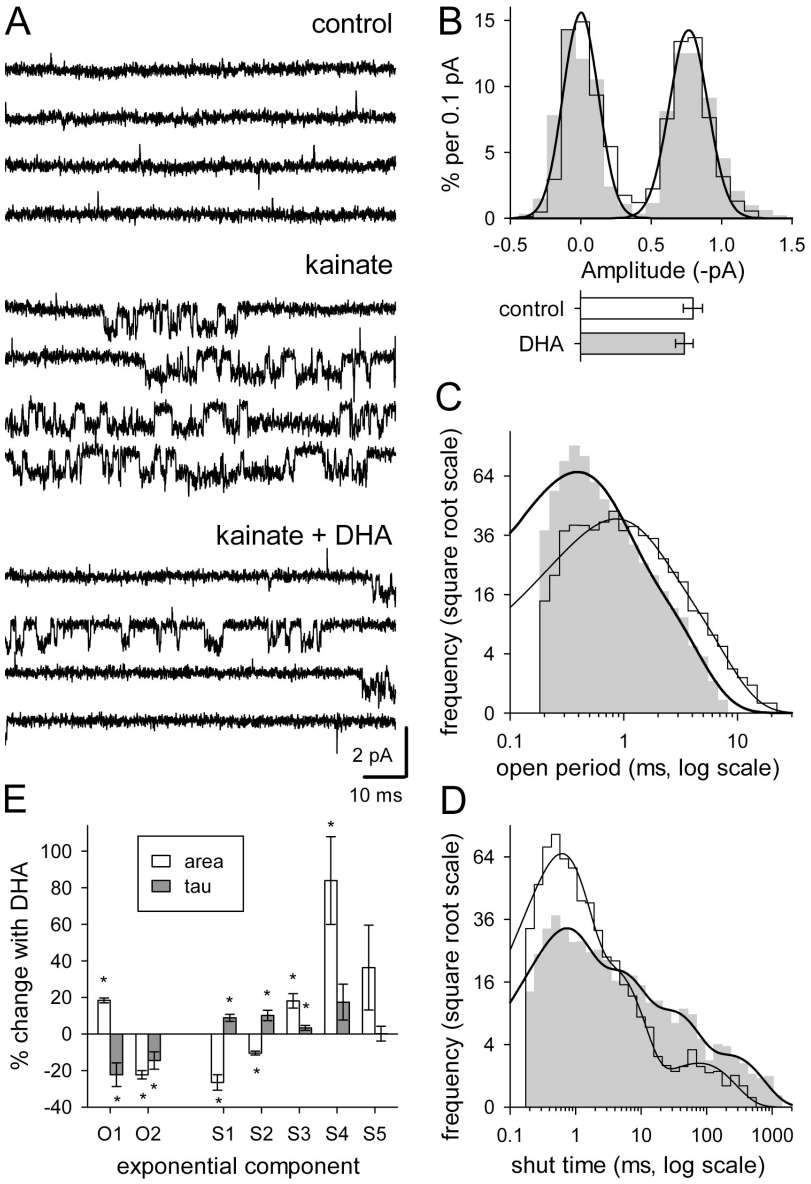

Figure 8. DHA reduces single channel open probability by increasing the prevalence of long duration shut times. (A) Each panel shows four continuous sweeps recorded in an outside-out patch from a cell transfected with GluR6(Q) T576R at a holding potential of −80 mV. No channel openings were observed in control external solution. Exposure to 10 μM kainate elicited channels with mean unitary current amplitude of 0.81 ± 0.07 pA (n = 9) (B), corresponding to a unitary conductance of 10.1 pS. When exposed simultaneously to kainate plus 15 μM DHA, the frequency of channel opening was dramatically reduced. Histograms of open (C) and shut (D) periods in the presence of 15 μM DHA (shaded plots) display an increase in the proportion of short duration open times and of long duration shut intervals as compared with the absence of DHA (open plots). Smooth curves are the best fit of a combination of exponential probability density functions. (E) Percent changes in the area and time constants for each exponential component derived from fits of open period histograms with two exponential components and closed time histograms with up to five components (data from nine patches).

of unitary currents but significantly reduced the open probability (0.53 ± 0.11 control; 0.12 ± 0.04 DHA, n = 9 patches) by increasing the prevalence of long duration shut times and of short duration open periods (Fig. 8).

Time Course of Desensitization

All of the experiments described thus far, including the single channel recordings, were performed on cells that had been exposed to the lectin concanavalin A (Con A), a treatment which dramatically increases steady-state currents mediated by recombinant kainate receptors (Partin et al., 1993) and by native kainate receptors in some, but not all types of neurons (Wilding and Huettner, 2001). Without Con A exposure, both GluR6(Q) and GluR6(R) homomeric receptors exhibit rapid and nearly complete desensitization. In addition, our previous work has shown that inhibition by DHA displays similar selectivity for the R versus the Q form of homomeric receptors when evaluated with or without Con A treatment, although the potency of DHA inhibition appears to be somewhat higher at receptors that have not been exposed to Con A (Wilding et al., 2005). To test whether any of the pore loop substitution mutations altered receptor desensitization and whether inhibition by DHA was correlated with the time course of current absent modification by Con A, we used rapid solution exchange to apply brief pulses of 300 μM kainate to transfected HEK cells that were not treated with Con A. As illustrated in Fig. S6 A, the different substitution mutant receptors desensitized at different rates and to different steady-state current levels. The summary plots in Fig. S6 (B–D) indicate that no significant correlation exists between susceptibility to DHA and either the onset or the steady-state level of desensitization.

Published June 18, 2008

DISCUSSION

We have used scanning mutagenesis to analyze the structural requirements for kainate receptor inhibition by the omega-3 fatty acid DHA. Our experiments focused on homomeric channels formed by wild-type or mutant versions of the GluR6 subunit expressed in HEK cells. In previous work, we showed that inhibition of wild-type receptors by DHA depends on mRNA editing at the Q/R site within the channel pore. Unedited subunits (Q590) resist inhibition, whereas channels in which all subunits derive from edited RNA (R590) are strongly inhibited (Wilding et al., 2005). Other investigators have shown that NMDA receptors, which have an asparagine (N) at the position homologous to the Q/R site, are potentiated by exposure to AA or DHA (Miller et al., 1992; Nishikawa et al., 1994). Our results in the present study support a number of different conclusions about the structural basis and mechanism of channel modulation by DHA. First, our experiments show that the presence of an N at position 590 is not sufficient for potentiation by DHA. Second, we find that strong inhibition by DHA is not precluded by the presence of a Q at this location and does not require the presence of a positively charged side chain at position 590 or at any other location within the pore. Thus, modulation cannot be explained by a simple interaction between DHA and the side chain at position 590. Instead, as discussed below, our results support the idea that susceptibility to inhibition by DHA likely depends on the conformation of the pore loop helix relative to the adjacent M1 and M3 transmembrane helices. In addition, our whole-cell fluctuation analysis and single channel recordings indicate that exposure to DHA does not reduce unitary conductance but significantly decreases channel open probability.

Pore Helix Conformation

By systematically introducing R substitutions at each residue of GluR6(Q) from V571 to P597 we detected a periodic pattern in the locations that confer susceptibility to DHA inhibition in the 15 amino acids immediately upstream of the Q/R site. Based on homology between glutamate receptors and potassium channel subunits this segment of the GluR6 pore loop is believed to form an α helix (Panchenko et al., 2001; Kuner et al., 2003). All of the upstream substitutions that allow for DHA inhibition of GluR6(Q) can be arranged along one side of this helix, while locations where R substitutions do not promote inhibition lie along the opposite side. In addition to structural predictions from homology modeling, previous analysis of NMDA and AMPA receptor subunits by the substituted cysteine accessibility method provides evidence about the orientation of the pore loop helix within channels of the glutamate receptor family (Kuner et al., 1996, 2001). Modification by methanethiosulfonate reagents applied from the cytoplasmic side of the membrane is restricted to cysteines substituted along one face of the upstream helix at positions −3 to −4, −7 to −8, −12 and >−14 relative to the Q/R site, essentially the same locations where R substitution fails to promote inhibition by DHA. Collectively, these results argue that this side of the helix faces away from the transmembrane helices that form the outer wall of the channel, and that R substitution along this face may have less of an impact on the pore loop conformation. In contrast, upstream locations where R substitutions confer susceptibility to DHA appear to be oriented away from the cytoplasm, toward the adjacent segments of M1 and M3 and the surrounding lipids (Fig. 9 and Fig. S2). In these locations either the size or the charge of the arginine side chain apparently perturbs the pore loop conformation in a way that is similar to the change introduced by Q to R editing at location 590. Understanding how this change in pore loop conformation translates into a difference in susceptibility to inhibition by DHA will require further study. A variety of evidence points to dynamic conformational changes in the pore loops of potassium channels (Liu et al., 1996; Cordero-Morales et al., 2007) and cyclic nucleotide-gated channels (Liu and Siegelbaum, 2000) that are thought to underlie physiological alterations in channel conductance or gating. Differential sensitivity of pore loop conformational changes to the local lipid environment could potentially explain the selective inhibition by DHA of wild-type GluR6(R), and the susceptible substitution mutants of GluR6(Q).

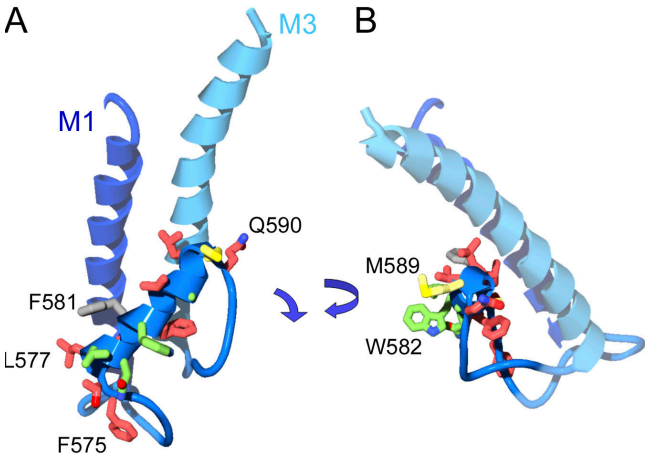

Figure 9. Substitutions that confer susceptibility to DHA lie along one face of the pore loop helix. (A and B) Homology model for M1-M3 region of GluR6(Q); cytoplasm to the bottom, extracellular space to the top of the figure. Amino acids in red exhibit inhibition by DHA when substituted to R in GluR6(Q), residues in green do not; yellow residues display intermediate inhibition. In B, the subunit was rotated and tilted, affording a view down the pore loop helix axis. Locations where R substitution enhances DHA inhibition are predicted to face toward the M1 and M3 helices.

Published June 18, 2008

Physiological Transition at the Q/R Site

At the structural level, the Q/R site is positioned at the transition between the upstream helix and the downstream open coil that forms the selectivity filter (Fig. S1 B). Functionally as well, the Q/R site appears to represent a transition point for several different aspects of channel operation. First, maximal whole-cell current was more severely reduced by substitutions at upstream locations, particularly those that conferred DHA susceptibility, than for wild-type editing to R590 or by R substitution at the +1 to +6 positions. Second, the unitary conductance and number of channels estimated from fluctuation analysis displayed an inverse relationship for upstream and downstream substitutions. As a group, the upstream substitutions exhibited relatively higher estimated conductance and lower channel number, whereas the opposite was true for GluR6(R) and the next six downstream R substitutions. Third, DHA inhibition of GluR6(Q) is entirely unaffected by R substitutions at the six downstream residues, yet strong inhibition results from substitution at the majority of locations up to 15 positions upstream. In this respect, wild-type edited GluR6 R590 matches the phenotype for upstream substitution, whereas in the other properties, channels with R at position 590 more closely resemble the downstream substitution mutants.

In addition to this transition in properties, there are some respects in which the Q/R site appears to be unique when compared with adjacent residues either upstream or downstream. For example, among the 39 subunits that we tested only those with positively charged R or K at position 590 displayed apparent permeability to chloride ions, as evidenced by a positive shift in reversal potential upon exchange of extracellular glucuronate for chloride. All six of the subunits with positive charge at position 590 shared this property. Positively charged R or K side chains extending from this location at the tip of each pore loop may have a greater impact on anion stability in the central cavity of the channel, possibly by counteracting the negative pore helix dipoles (Doyle et al., 1998), than would charged residues upstream or downstream of the apex.

Expression of Mutant Channels

Structure–function studies of potassium channels have shown that many pore loop substitutions result in a loss of functional channel expression. Some point mutations in the pore loop disrupt subunit tetramerization (Heginbotham et al., 1997), whereas in other cases channels are delivered to the cell surface, as determined by voltage-dependent gating charge movement, but potassium ion conduction through the pore is eliminated (Perozo et al., 1993). Glutamate receptor channels appear to tolerate a larger repertoire of substitutions, possibly owing to their larger pore dimensions. Estimates of pore size at the selectivity filter based on permeation of organic cations suggest a diameter of ~5.5 Å for NMDA receptors (Villarroel et al., 1995), 7.5–7.6 Å for both Q and R forms of kainate receptors and ~7.8 Å for AMPA receptors (Burnashev et al., 1996). In contrast, potassium channels exhibit a narrower pore diameter of ~3 Å (Hille, 2001). With some notable exceptions, single amino acid substitutions involving small or hydrophobic side chains in the pore loops of NMDA (Kuner et al., 1996; Williams et al., 1998; Kashiwagi et al., 2002), AMPA (Kuner et al., 2001), and kainate (Panchenko et al., 1999; 2001) receptor subunits yield functional channels. On the other hand, cation-selective cyclic nucleotide-gated channels have an estimated pore diameter in the range of 5.8 to 6.4 Å (Goulding et al., 1993), yet scanning mutagenesis of bovine rod cGMP-gated channels revealed that cysteine substitution abrogated channel expression (Sun et al., 1996) or dramatically reduced open probability (Becchetti and Gamel, 1999) at more than half of all pore loop residues. Therefore, pore size alone may not entirely explain the ability of glutamate receptors to tolerate side chain substitutions.

Before undertaking our scan we were concerned that the larger size and positive charge of the arginine side chain might be tolerated less well than smaller or more hydrophobic residues. Indeed, homomeric tetramerization of AMPA receptor subunits is known to be disfavored by the presence of R at the Q/R site or at several other positions in the pore loop (Greger et al., 2003), providing an explanation for the meager current amplitude when GluR2(R) is expressed alone (e.g., Burnashev et al., 1996). In addition, R substitution at position M589 of GluR6, or at several locations in AMPA receptor subunits GluR1 (M located −1 relative to the Q/R site) or GluR3 (M and A, −1 and −3 residues relative to the Q/R site, respectively), was shown to exert a dominant-negative phenotype. The mutant subunits exhibited very little current when expressed alone and suppressed currents mediated by wild-type subunits in neurons and in cotransfected heterologous cells (Dingledine et al., 1992; Robert et al., 2002). Our results are broadly consistent with these earlier studies. Several of the R substitution mutants, particularly those susceptible to DHA inhibition, displayed lower maximal whole-cell current amplitudes and lower estimated channel number than for wild-type GluR6(Q), suggesting reduced delivery or stability of these channels at the plasma membrane. Following treatment with Con A we were able to record sufficient current to analyze DHA inhibition for all but one of the R substitutions (F581R), however we noted that for several of the mutants (F575R, S580R, F581R, G584R, M589R, and P597R) kainate evoked very little current (<100 pA) without prior exposure to Con A (compared with >200 pA for all but F581R after Con A). Importantly, this trend for smaller currents does not hold for homomeric channels formed by wild-type edited subunits or for unedited subunits

with R substitutions at positions 591–596. Cells expressing GluR6(R) display robust kainate-evoked currents (Partin et al., 1993) and our fluctuation analysis indicates a higher level of surface expression for GluR6(R) than for GluR6(Q), suggesting that future experiments to examine the trafficking of edited, unedited, and mutant versions of GluR6 should be informative.

Lipid–Protein Interactions

It is not yet known exactly how the functional properties of ion channels and other membrane proteins are regulated by AA and DHA or by other lipid-derived modulators such as lysophospholipids (Patel et al., 2001). Mechanisms involving relatively large-scale deformations such as changes in elasticity (Bruno et al., 2007), curvature, and lateral tension (Patel et al., 2001) have been proposed to account for the gating of mechanosensitive channels as well as for the modulation of NMDA receptors by DHA (Casado and Ascher, 1998). On the other hand, a variety of studies suggest that bulk lipids exert substantially less influence on the function of membrane proteins than do annular lipids, which directly surround and contact the protein (Powl and Lee, 2007). Crystal structures of bacterial (Valiyaveetil et al., 2002) and mammalian (Long et al., 2007) potassium channels include partially resolved lipids, indicating that close interactions with the protein surface are sufficient to constrain the inherent disorder of alkyl chains. Indeed, detergent-purified KcsA channels include phosphatidylglycerol in contact with the pore helix and downstream M2 helix at the interface between each subunit. In addition, the presence of phospholipid is required for proper refolding of fully denatured KcsA subunits, and negatively charged phospholipids are necessary for functional reconstitution (Valiyaveetil et al., 2002). Thus, specific lipid interactions can have a direct impact on the structural integrity and operation of channel proteins.

Neuronal membranes are particularly rich in lipids that include cis-unsaturated fatty acyl chains, typically at the sn-2 position. Studies of synaptosomes and retinal membranes indicate >30% DHA content in gray matter phosphatidylethanolamine and phosphatidylserine (Salem et al., 2001). Recent molecular modeling studies highlight the dynamic flexibility of DHA relative to saturated alkyl chains (Zimmerberg and Gawrisch, 2006), which may underlie the preferential ability of DHA-containing lipids to conform to the uneven outer surface of membrane-embedded proteins and to modify associations between adjacent helices (Grossfield et al., 2006). The physiological effects of free DHA, whether delivered experimentally or liberated by endogenous phospholipase activity (Farooqui et al., 2006), may result from displacement of annular lipids or from a distinct mode of association that cannot be attained when DHA is constrained as part of an intact lipid molecule.

We are grateful to David Sept for advice on homology modeling, to Colin Nichols, Decha Enkvetchakul, and Fernanda Laezza for critical reading of the manuscript, to Steve Heinemann for providing channel subunit cDNAs, and to David Clapham for L3T4 cDNA.

This work was supported by the National Institutes of Health (NS30888).

Olaf S. Andersen served as editor.

Submitted: 25 March 2008
Accepted: 15 May 2008

REFERENCES

Armstrong, N., Y. Sun, G.Q. Chen, and E. Gouaux. 1998. Structure of a glutamate-receptor ligand-binding core in complex with kainate. *Nature.* 395:913–917.

Becchetti, A., and K. Gamel. 1999. The properties of cysteine mutants in the pore region of cyclic-nucleotide-gated channels. *Pflugers Arch.* 438:587–596.

Bowie, D., and M.L. Mayer. 1995. Inward rectification of both AMPA and kainate subtype glutamate receptors generated by polyamine-mediated ion channel block. *Neuron.* 15:453–462.

Bruno, M.J., R.E. Koeppe II, and O.S. Andersen. 2007. Docosahexaenoic acid alters bilayer elastic properties. *Proc. Natl. Acad. Sci. USA.* 104:9638–9643.

Burnashev, N., Z. Zhou, E. Neher, and B. Sakmann. 1995. Fractional calcium currents through recombinant GluR channels of the NMDA, AMPA and kainate receptor subtypes. *J. Physiol.* 485:403–418.

Burnashev, N., A. Villarroel, and B. Sakmann. 1996. Dimensions and ion selectivity of recombinant AMPA and kainate receptor channels and their dependence on Q/R site residues. *J. Physiol.* 496:165–173.

Casado, M., and P. Ascher. 1998. Opposite modulation of NMDA receptors by lysophospholipids and arachidonic acid: common features with mechanosensitivity. *J. Physiol.* 513:317–330.

Cordero-Morales, J.F., V. Jogini, A. Lewis, V. Vásquez, D.M. Cortes, B. Roux, and E. Perozo. 2007. Molecular driving forces determining potassium channel slow inactivation. *Nat. Struct. Mol. Biol.* 14:1062–1069.

Dingledine, R., R.I. Hume, and S.F. Heinemann. 1992. Structural determinants of barium permeation and rectification in non-NMDA glutamate receptor channels. *J. Neurosci.* 12:4080–4087.

Dingledine, R., K. Borges, D. Bowie, and S.F. Traynelis. 1999. The glutamate receptor ion channels. *Pharmacol. Rev.* 51:7–61.

Doyle, D.A., J. Morais Cabral, R.A. Pfuetzner, A. Kuo, J.M. Gulbis, S.L. Cohen, B.T. Chait, and R. MacKinnon. 1998. The structure of the potassium channel: molecular basis of K^+ conduction and selectivity. *Science.* 280:69–77.

Egebjerg, J., B. Bettler, I. Hermans-Borgmeyer, and S. Heinemann. 1991. Cloning of a cDNA for a glutamate receptor subunit activated by kainate but not AMPA. *Nature.* 351:745–748.

Farooqui, A.A., W.Y. Ong, and L.A. Horrocks. 2006. Inhibitors of brain phospholipase A2 activity: their neuropharmacological effects and therapeutic importance for the treatment of neurologic disorders. *Pharmacol. Rev.* 58:591–620.

Fink, M., F. Lesage, F. Duprat, C. Heurteaux, R. Reyes, M. Fosset, and M. Lazdunski. 1998. A neuronal two P domain K^+ channel stimulated by arachidonic acid and polyunsaturated fatty acids. *EMBO J.* 17:3297–3308.

Gebhardt, C., and S.G. Cull-Candy. 2006. Influence of agonist concentration on AMPA and kainate channels in CA1 pyramidal cells in rat hippocampal slices. *J. Physiol.* 573:371–394.

Goulding, E.H., G.R. Tibbs, D. Liu, and S.A. Siegelbaum. 1993. Role of H5 domain in determining pore diameter and ion permeation through cyclic nucleotide-gated channels. *Nature.* 364:61–64.

Greger, I.H., L. Khatri, X. Kong, and E.B. Ziff. 2003. AMPA receptor tetramerization is mediated by Q/R editing. *Neuron.* 40:763–774.

Grossfield, A., S.E. Feller, and M.C. Pitman. 2006. A role for direct interactions in the modulation of rhodopsin by omega-3 polyunsaturated lipids. *Proc. Natl. Acad. Sci. USA.* 103:4888–4893.

Heginbotham, L., E. Odessey, and C. Miller. 1997. Tetrameric stoichiometry of a prokaryotic K^+ channel. *Biochemistry.* 36:10335–10342.

Hille, B. 2001. Ion Channels of Excitable Membranes. Third ed. Sinauer Associates, Inc., Sunderland, MA. 814 pp.

Hollmann, M., and S. Heinemann. 1994. Cloned glutamate receptors. *Annu. Rev. Neurosci.* 17:31–108.

Howe, J.R. 1996. Homomeric and heteromeric ion channels formed from the kainate-type subunits GluR6 and KA2 have very small, but different, unitary conductances. *J. Neurophysiol.* 76:510–519.

Huettner, J.E. 1990. Glutamate receptor channels in rat DRG neurons: activation by kainate and quisqualate blockade of desensitization by Con A. *Neuron.* 5:255–266.

Huettner, J.E., E. Stack, and T.J. Wilding. 1998. Antagonism of neuronal kainate receptors by lanthanum and gadolinium. *Neuropharmacology.* 37:1239–1247.

Kamboj, S.K., G.T. Swanson, and S.G. Cull-Candy. 1995. Intracellular spermine confers rectification on rat calcium-permeable AMPA and kainate receptors. *J. Physiol.* 486:297–303.

Kashiwagi, K., T. Masuko, C.D. Nguyen, T. Kuno, I. Tanaka, K. Igarashi, and K. Williams. 2002. Channel blockers acting at *N*-methyl-D-aspartate receptors: differential effects of mutations in the vestibule and ion channel pore. *Mol. Pharmacol.* 61:533–545.

Keinänen, K., W. Wisden, B. Sommer, P. Werner, A. Herb, T.A. Verdoorn, B. Sakmann, and P.H. Seeburg. 1990. A family of AMPA-selective glutamate receptors. *Science.* 249:556–560.

Köhler, M., N. Burnashev, B. Sakmann, and P.H. Seeburg. 1993. Determinants of Ca^{2+} permeability in both TM1 and TM2 of high affinity kainate receptor channels: Diversity by RNA editing. *Neuron.* 10:491–500.

Kuner, T., P.H. Seeburg, and H.R. Guy. 2003. A common architecture for K^+ channels and ionotropic glutamate receptors? *Trends Neurosci.* 26:27–32.

Kuner, T., C. Beck, B. Sakmann, and P.H. Seeburg. 2001. Channel-lining residues of the AMPA receptor M2 segment: structural environment of the Q/R site and identification of the selectivity filter. *J. Neurosci.* 21:4162–4172.

Kuner, T., L.P. Wollmuth, A. Karlin, P.H. Seeburg, and B. Sakmann. 1996. Structure of the NMDA receptor channel M2 segment inferred from the accessibility of substituted cysteines. *Neuron.* 17:343–352.

Kuo, A., J.M. Gulbis, J.F. Antcliff, T. Rahman, E.D. Lowe, J. Zimmer, J. Cuthbertson, F.M. Ashcroft, T. Ezaki, and D.A. Doyle. 2003. Crystal structure of the potassium channel KirBac1.1 in the closed state. *Science.* 300:1922–1926.

Kutsuwada, T., N. Kashiwabuchi, H. Mori, K. Sakimura, E. Kushiya, K. Araki, H. Meguro, H. Masaki, T. Kumanishi, M. Arakawa, and M. Mishina. 1992. Molecular diversity of the NMDA receptor channel. *Nature.* 358:36–41.

Lee, S.Y., A. Lee, J. Chen, and R. Mackinnon. 2005. Structure of the KvAP voltage-dependent K^+ channel and its dependence on the lipid membrane. . *Proc. Natl. Acad. Sci. USA.* 102:15441–15446.

Liu, Y., M.E. Jurman, and G. Yellen. 1996. Dynamic rearrangement of the outer mouth of a K^+ channel during gating. *Neuron.* 16:859–867.

Liu, J., and S.A. Siegelbaum. 2000. Change of pore helix conformational state upon opening of cyclic nucleotide-gated channels. *Neuron.* 28:899–909.

Long, S.B., E.B. Campbell, and R. Mackinnon. 2005. Crystal structure of a mammalian voltage-dependent Shaker family K^+ channel. *Science.* 309:897–903.

Long, S.B., X. Tao, E.B. Campbell, and R. MacKinnon. 2007. Atomic structure of a voltage-dependent K^+ channel in a lipid membrane-like environment. *Nature.* 450:376–382.

Miller, B., M. Sarantis, S.F. Traynelis, and D. Attwell. 1992. Potentiation of NMDA receptor currents by arachidonic acid. *Nature.* 355:722–725.

Mayer, M.L. 2005. Crystal structures of the GluR5 and GluR6 ligand binding cores: molecular mechanisms underlying kainate receptor selectivity. *Neuron.* 45:539–552.

Monyer, H., R. Sprengel, R. Schoepfer, A. Herb, M. Higuchi, H. Lomeli, N. Burnashev, B. Sakmann, and P.H. Seeburg. 1992. Heteromeric NMDA receptors: molecular and functional distinction of subtypes. *Science.* 256:1217–1221.

Moriyoshi, K., M. Masu, T. Ishii, R. Shigemoto, N. Mizuno, and N. Nakanishi. 1991. Molecular cloning and characterization of the rat NMDA receptor. *Nature.* 354:31–37.

Nishikawa, M., S. Kimura, and N. Akaike. 1994. Facilitatory effect of docosahexaenoic acid on *N*-methyl-D-aspartate response in pyramidal neurones of rat cerebral cortex. *J. Physiol.* 475:83–93.

Oliver, D., C.C. Lien, M. Soom, T. Baukrowitz, P. Jonas, and B. Fakler. 2004. Functional conversion between A-type and delayed rectifier K^+ channels by membrane lipids. *Science.* 304:265–270.

Panchenko, V.A., C.R. Glasser, K.M. Partin, and M.L. Mayer. 1999. Amino acid substitutions in the pore of rat glutamate receptors at sites influencing block by polyamines. *J. Physiol.* 520:337–357.

Panchenko, V.A., C.R. Glasser, and M.L. Mayer. 2001. Structural similarities between glutamate receptor channels and K^+ channels examined by scanning mutagenesis. *J. Gen. Physiol.* 117:345–360.

Partin, K.M., D.K. Patneau, C.A. Winters, M.L. Mayer, and A. Buonanno. 1993. Selective modulation of desensitization at AMPA versus kainate receptors by cyclothiazide and concanavalin A. *Neuron.* 11:1069–1082.

Patel, A.J., M. Lazdunski, and E. Honoré. 2001. Lipid and mechano-gated 2P domain K^+ channels. *Curr. Opin. Cell Biol.* 13:422–428.

Perozo, E., R. MacKinnon, F. Bezanilla, and E. Stefani. 1993. Gating currents from a nonconducting mutant reveal open-closed conformations in Shaker K^+ channels. *Neuron.* 11:353–358.

Poling, J.S., S. Vicini, M.A. Rogawski, and N. Salem Jr. 1996. Docosahexaenoic acid block of neuronal voltage-gated K^+ channels: subunit selective antagonism by zinc. *Neuropharmacology.* 35:969–982.

Powl, A.M., and A.G. Lee. 2007. Lipid effects on mechanosensitive channels. *Current Topics in Membranes.* 58:151–178.

Robert, A., R. Hyde, T.E. Hughes, and J.R. Howe. 2002. The expression of dominant-negative subunits selectively suppresses neuronal AMPA and kainate receptors. *Neuroscience.* 115:1199–1210.

Salem, N. Jr., B. Litman, H.Y. Kim, and K. Gawrisch. 2001. Mechanisms of action of docosahexaenoic acid in the nervous system. *Lipids.* 36:945–959.

Sali, A., and T.L. Blundell. 1993. Comparative protein modeling by satisfaction of spatial restraints. *J. Mol. Biol.* 234:779–815.

Schrempf, H., O. Schmidt, R. Kummerlen, S. Hinnah, D. Muller, M. Betzler, T. Steinkamp, and R. Wagner. 1995. A prokaryotic potassium ion channel with two predicted transmembrane segments from *Streptomyces lividans. EMBO J.* 14:5170–5178.

Sigworth, F.J. 1980. The variance of sodium current fluctuations at the node of Ranvier. *J. Physiol.* 307:97–129.

Smith, T.C., and J.R. Howe. 2000. Concentration-dependent substate behavior of native AMPA receptors. *Nat. Neurosci.* 3:992–997.

Sommer, B., M. Kohler, R. Sprengel, and P.H. Seeburg. 1991. RNA editing in brain controls a determinant of ion flow in glutamate-gated channels. *Cell.* 67:11–19.

Sun, Z.P., M.H. Akabas, E.H. Goulding, A. Karlin, and S.A. Siegelbaum. 1996. Exposure of residues in the cyclic nucleotide-gated channel pore: P region structure and function in gating. *Neuron.* 16:141–149.

Swanson, G.T., D. Feldmeyer, M. Kaneda, and S.G. Cull-Candy. 1996. Effect of RNA editing and subunit co-assembly on single-channel properties of recombinant kainate receptors. *J. Physiol.* 492:129–142.

Published June 18, 2008

Traynelis, S.F., and F. Jaramillo. 1998. Getting the most out of noise in the central nervous system. *Trends Neurosci.* 21:137–145.

Valiyaveetil, F.I., Y. Zhou, and R. MacKinnon. 2002. Lipids in the structure, folding, and function of the KcsA K^+ channel. *Biochemistry.* 41:10771–10777.

Villarroel, A., N. Burnashev, and B. Sakmann. 1995. Dimensions of the narrow portion of a recombinant NMDA receptor channel. *Biophys. J.* 68:866–875.

Wilding, T.J., Y.H. Chai, and J.E. Huettner. 1998. Inhibition of rat neuronal kainate receptors by cis-unsaturated fatty acids. *J. Physiol.* 513:331–339.

Wilding, T.J., and J.E. Huettner. 2001. Functional diversity and developmental changes in neuronal kainate receptors. *J. Physiol.* 532:411–421.

Wilding, T.J., Y. Zhou, and J.E. Huettner. 2005. Q/R site editing controls kainate receptor inhibition by membrane fatty acids. *J. Neurosci.* 25:9470–9478.

Williams, K., A.J. Pahk, K. Kashiwagi, T. Masuko, N.D. Nguyen, and K. Igarashi. 1998. The selectivity filter of the *N*-methyl-D-aspartate receptor: a tryptophan residue controls block and permeation of Mg^{2+}. *Mol. Pharmacol.* 53:933–941.

Wollmuth, L.P., and A.I. Sobolevsky. 2004. Structure and gating of the glutamate receptor ion channel. *Trends Neurosci.* 27:321–328.

Wo, Z.G., and R.E. Oswald. 1995. Unraveling the modular design of glutamate-gated ion channels. *Trends Neurosci.* 18:161–168.

Wood, M.W., H.M. VanDongen, and A.M. VanDongen. 1995. Structural conservation of ion conduction pathways in K channels and glutamate receptors. *Proc. Natl. Acad. Sci. USA.* 92:4882–4886.

Zhou, Y., and R. MacKinnon. 2003. The occupancy of ions in the K^+ selectivity filter: charge balance and coupling of ion binding to a protein conformational change underlie high conduction rates. *J. Mol. Biol.* 333:965–975.

Zimmerberg, J., and K. Gawrisch. 2006. The physical chemistry of biological membranes. *Nat. Chem. Biol.* 2:564–567.

Online Supplemental Material

Figure S1. Sequence alignment and homology model.
(**A**) Alignment of GluR6 to KcsA (1R3J, Zhou and MacKinnon, 2003), KirBac1.1 (1P7B, Kuo et al., 2003), KvAP (2A0L, Lee et al., 2005) and Kv1.2 (2A79, Long et al., 2005) that were used as simultaneous templates. Color code for identical and similar residues (see Kuner et al., 2003): Yellow = Identical to GluR6 sequence; Grey = Small (G, A, S, T, C, P); Green = Aromatic (F, Y, W); Light Blue = Alkyl (V, I, L, M); Red = Negative (D, E); Dark Blue = Positive (K, R, H). (**B**) Models of GluR6(Q) subunit secondary structure based on homology with X-ray diffraction structures of the 4 potassium channel subunits in panel (**A**). The Q side chain at position 590 is illustrated on two opposite subunits from the channel tetramer; cytoplasm to the bottom, extracellular space to the top of the figure.

Figure S2. Channel homology model with associated lipids. Channel tetramers alone (*left*), or with lipid residues from the potassium channel crystal structure of Long et al. (2007) PDB entry 2R9R (*right*), as viewed from the side (**A**), or from the extracellular (**B**) or intracellular (**C**) side of the membrane. The third transmembrane (M4) helix and the extracellular agonist-binding domain were not modeled and are not illustrated.

Figure S3. Edited residues in TM1 do not affect inhibition of homomeric GluR6(R) or (Q). Fractional inhibition of kainate-evoked current by DHA plotted for single point mutants V536I and C540Y of GluR6(R) and GluR6(Q) (n=5 to 7 cells per construct).

Figure S4. Inhibition correlates with mean control current amplitude. (**A**) Control current amplitude, normalized to the mean value obtained for GluR6(Q), plotted for each of the pore-loop R substitution mutants. (**B**) Fractional inhibition by DHA (I / Icontrol) plotted versus normalized control current amplitude for all of the tested constructs (n=5 to 32 cells per construct). Pearson Product Moment Correlation Coefficient = 0.780, $p<0.001$. Straight line is the best fit linear regression through the origin. (**C**) Points show the mean values from panel **B**; straight colored lines span the range of normalized current values with the best fit slope to all data points for each construct. The regression line from panel **B** is re-plotted and the dashed black line is for wild-type GluR6(Q).

Figure S5. Individual mutations do not exhibit cell-by-cell correlation between DHA inhibition and control current amplitude. For each of the wild-type and mutant subunits the Pearson product moment correlation coefficient (PPMCC) was calculated and plotted on the abscissa. An index of statistical significance, 1-p for the PPMCC, is plotted on the ordinate. Only points that fall above the dashed line at 0.95 indicate significant correlation among the cells for that particular construct (n=5-32 cells per construct).

Figure S6. Extent and time course of desensitization do not correlate with susceptibility to inhibition by DHA. (**A**) Sample whole-cell currents evoked by rapid application of 300 µM kainate to HEK cells transfected with GluR6(R) or one of six GluR6(Q) mutants bearing an R substitution elsewhere in the pore-loop. None of the cells were exposed to Con A. (**B**) Summary plot of steady-state / peak ratio for the R substitutions (n = 3 to 29 cells per construct). (**C**) Plots of fractional inhibition by DHA (I / Icontrol) versus the SS / peak ratio (large symbols) and versus the fraction of current decay described by the faster of two exponential components (small symbols) from the best fit of two exponentials plus a constant. (**D**) Fractional inhibition by DHA (I / Icontrol) plotted versus the time constants (Tau 1 & 2) for the fast and slow exponential components. Many substitutions upstream of the Q/R site reduced the rate or the extent of whole-cell current desensitization irrespective of effect on DHA inhibition; downstream substitutions had less effect on desensitization.

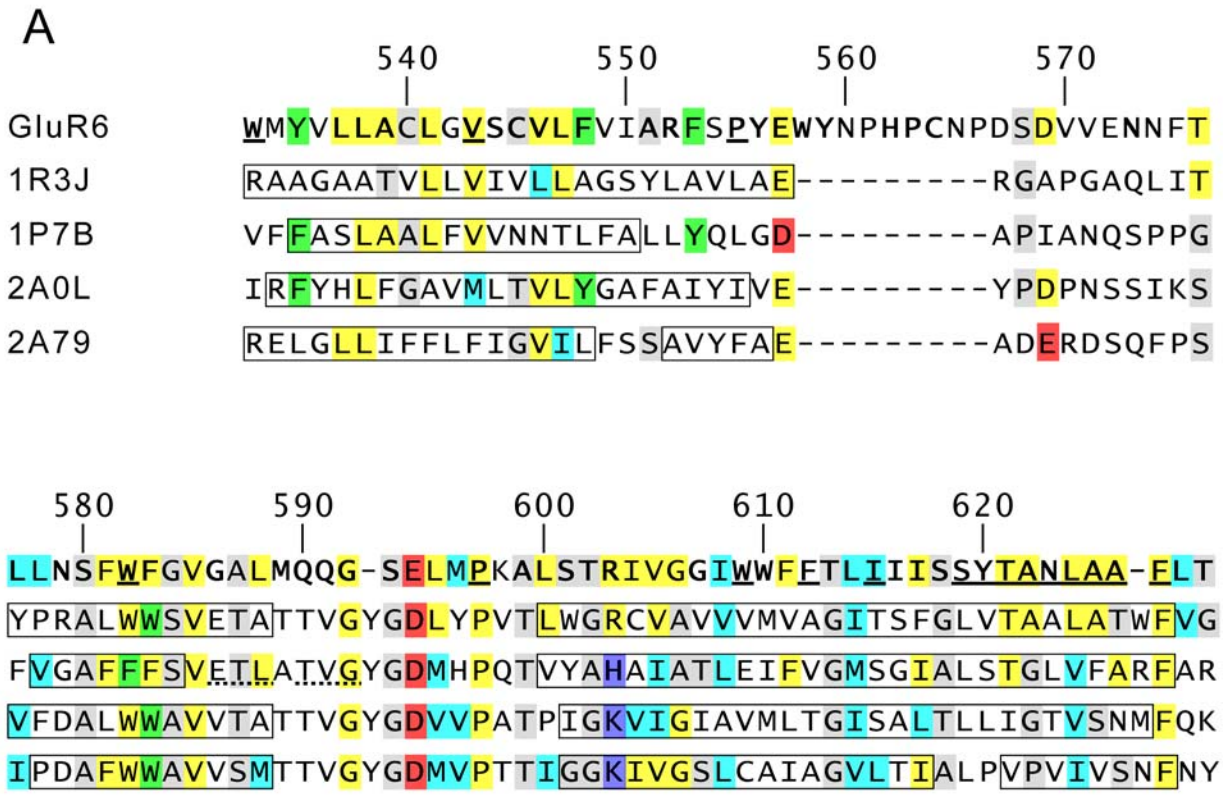
A
540
550
560
570
GluR6
1R3J
1P7B
2A0L
2A79
580
590
600
610
620

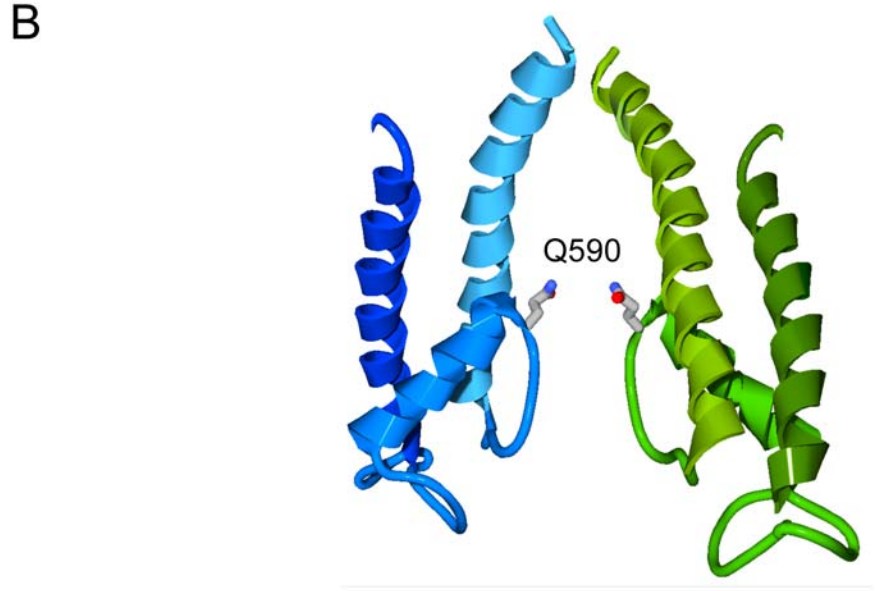
B
Q590

Figure S1

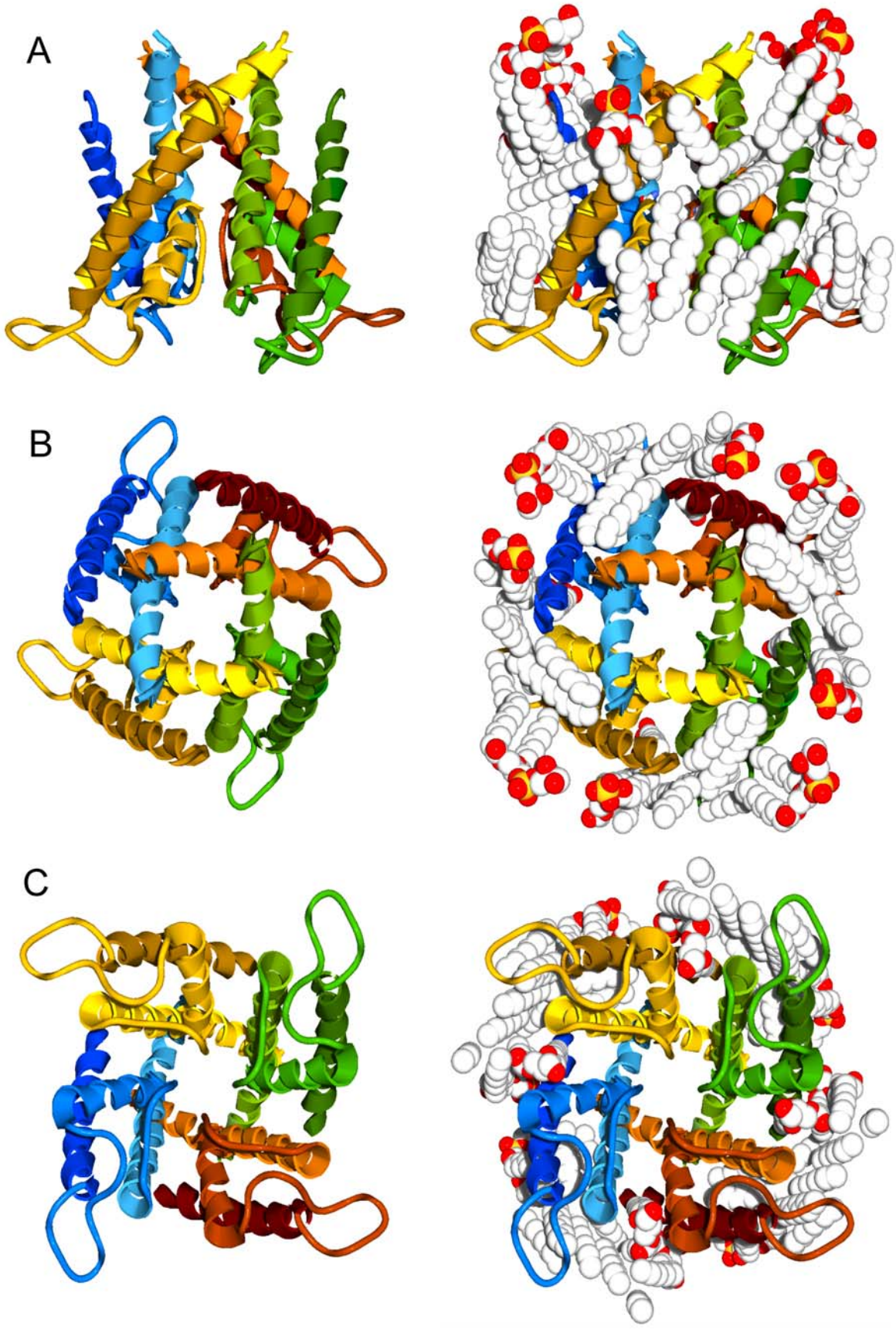

Figure S2

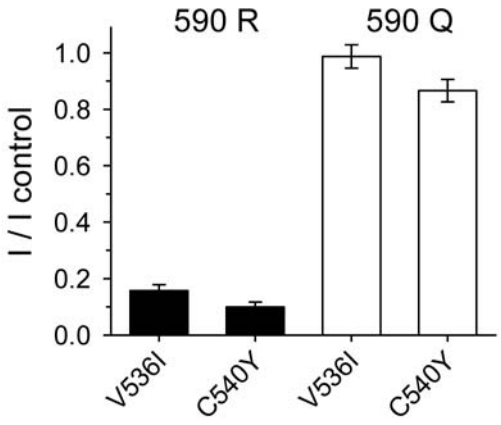

Figure S3

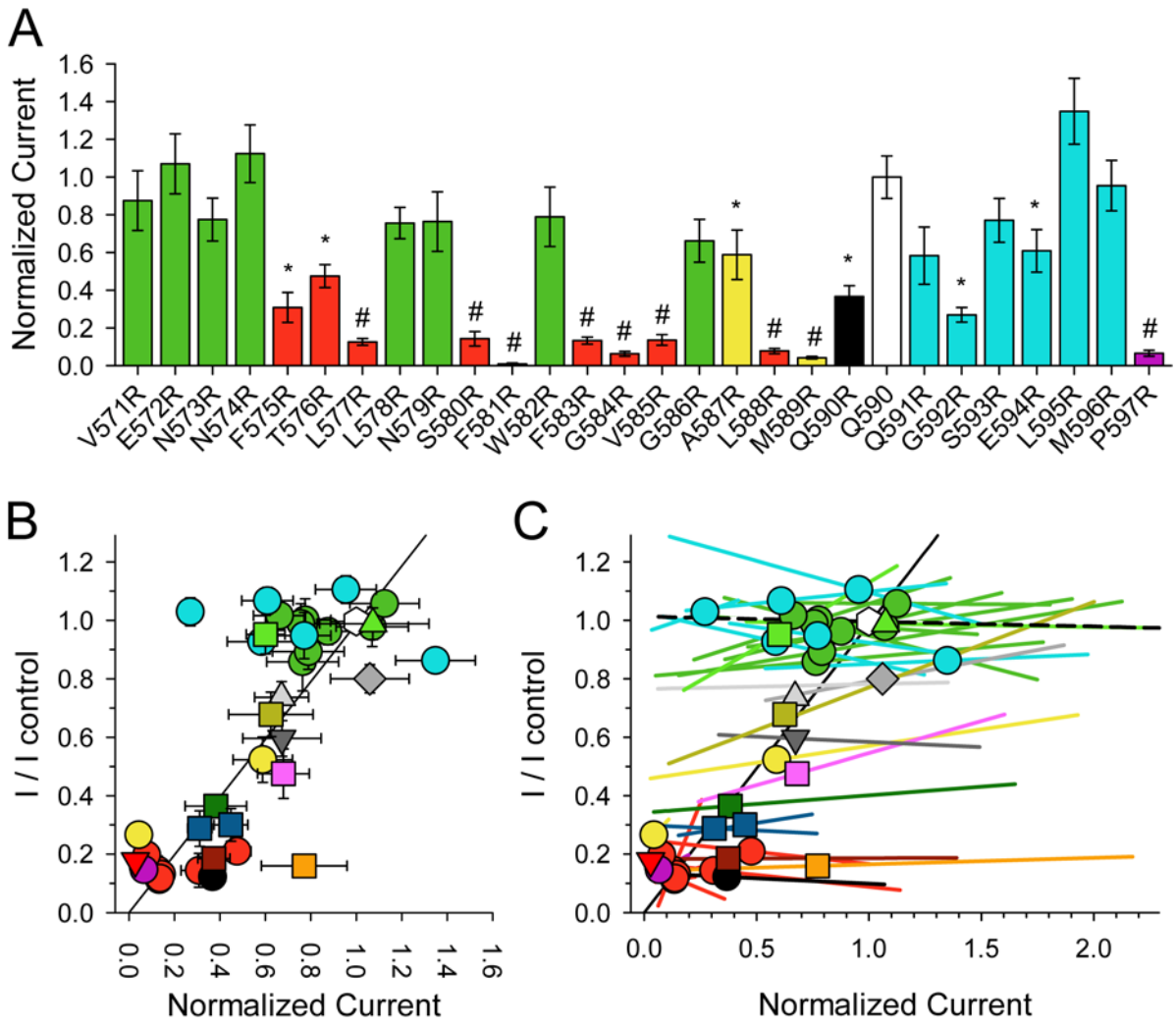
A
Normalized Current
1.6
1.4
1.2
1.0
0.8
0.6
0.4
0.2
0.0
V571R
E572R
N573R
N574R
F575R
T576R
L577R
L578R
N579R
S580R
F581R
W582R
F583R
G584R
V585R
G586R
A587R
L588R
M589R
Q590R
Q590
Q591R
G592R
S593R
E594R
L595R
M596R
P597R
B
I / I control
Normalized Current
C
I / I control
Normalized Current

Figure S4

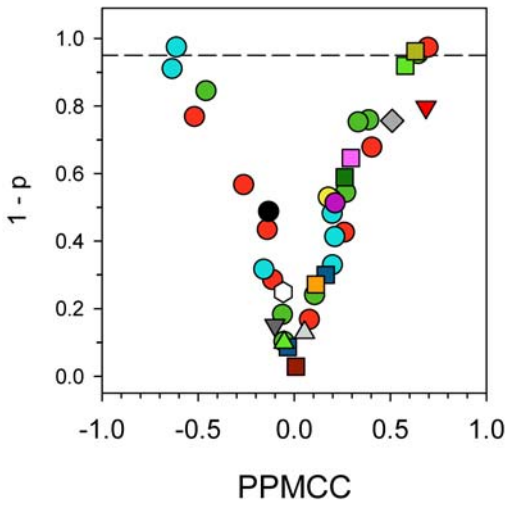

Figure S5

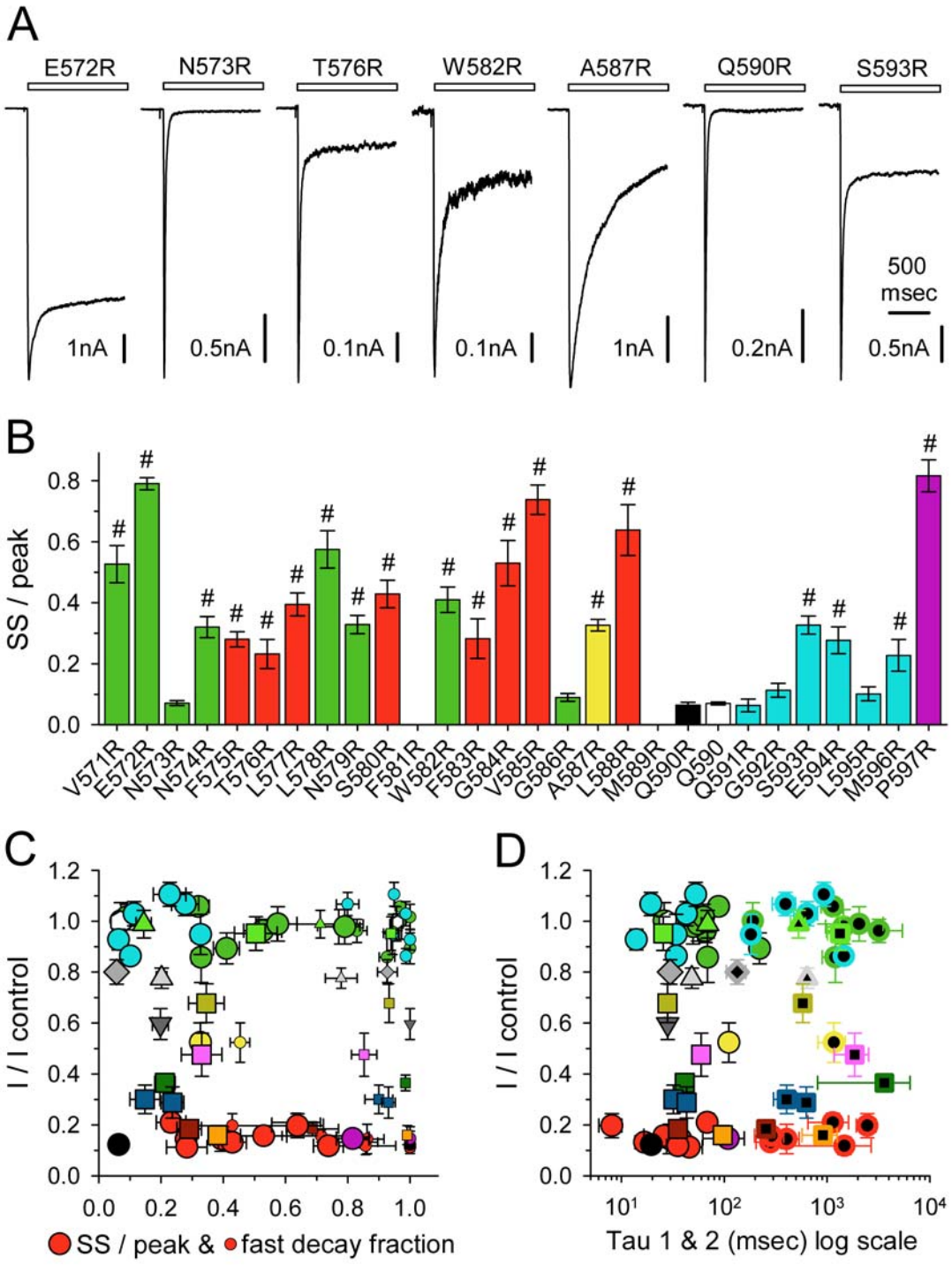
A
E572R
N573R
T576R
W582R
A587R
Q590R
S593R
1nA
0.5nA
0.1nA
0.1nA
1nA
0.2nA
0.5nA
500 msec
B
SS / peak
0.0
0.2
0.4
0.6
0.8
V571R
E572R
N573R
N574R
F575R
T576R
L577R
L578R
N579R
S580R
F581R
W582R
F583R
G584R
V585R
G586R
A587R
L588R
M589R
Q590R
Q590
Q591R
G592R
S593R
E594R
L595R
M596R
P597R
C
I / I control
0.0
0.2
0.4
0.6
0.8
1.0
1.2
SS / peak & fast decay fraction
D
I / I control
Tau 1 & 2 (msec) log scale
10¹
10²
10³
10⁴

Figure S6